AD-A066 534 AERONAUTICAL RESEARCH LABS MELBOURNE (AUSTRALIA) F/G 13/9
STEADY STATE BEHAVIOUR OF A CABLE USED FOR SUSPENDING A SONAR B--ETC(U)
MAY 78 N E GILBERT

UNCLASSIFIED ARL/AERO-149 NL

| OF |
AD
A066534

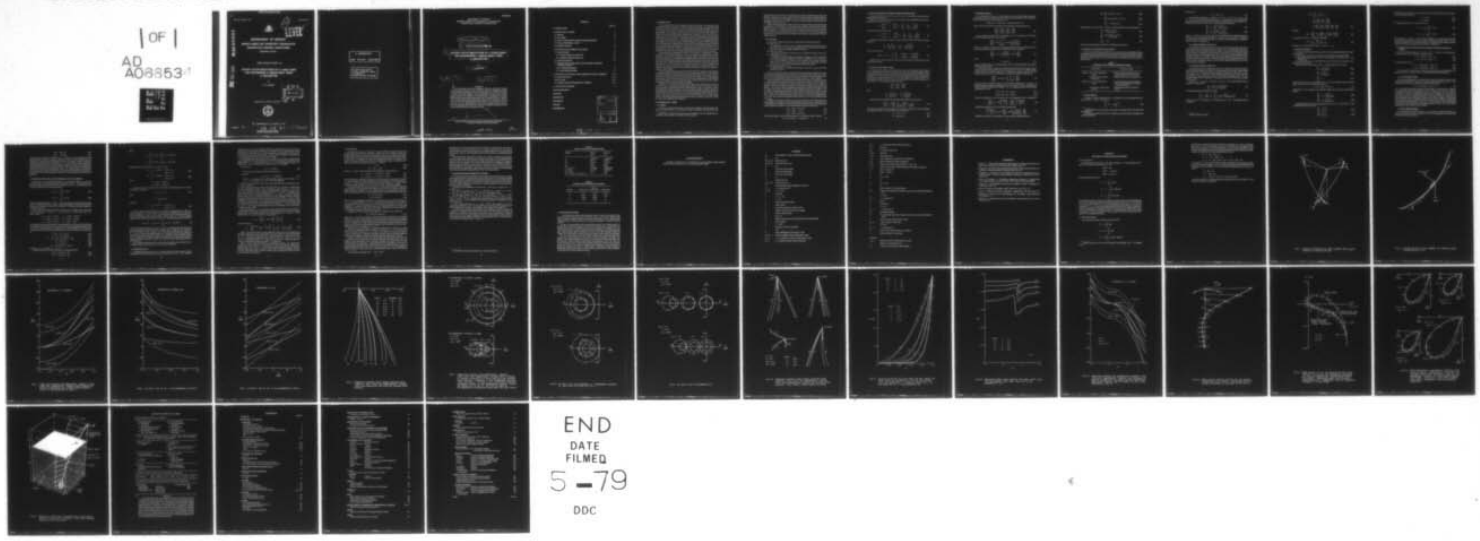

END
DATE
FILMED
5-79
DDC

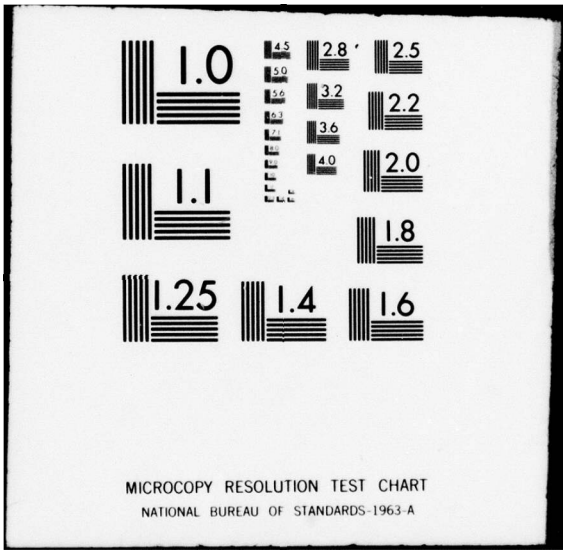
1.0
1.1
1.25
1.4
1.6
1.8
2.0
2.2
2.5
2.8
3.2
3.6
4.0
4.5
5.0
5.6
6.3
MICROCOPY RESOLUTION TEST CHART
NATIONAL BUREAU OF STANDARDS-1963-A

ARL-Aero-Report-149

AR-001-269

LEVEL

DEPARTMENT OF DEFENCE

DEFENCE SCIENCE AND TECHNOLOGY ORGANISATION

AERONAUTICAL RESEARCH LABORATORIES

MELBOURNE, VICTORIA

AERODYNAMICS REPORT 149

STEADY STATE BEHAVIOUR OF A CABLE USED FOR SUSPENDING A SONAR BODY FROM A HELICOPTER

by

N. E. GILBERT

Approved for Public Release

COPY No 17

79 03 29 033

May 1978

AR-001-269

DEPARTMENT OF DEFENCE
DEFENCE SCIENCE AND TECHNOLOGY ORGANISATION
AERONAUTICAL RESEARCH LABORATORIES

(14) ARL/AERO-149

(9) AERODYNAMICS REPORT 149

(6) STEADY STATE BEHAVIOUR OF A CABLE USED FOR SUSPENDING A SONAR BODY FROM A HELICOPTER.

by

(10) N. E. GILBERT

(11) May 78

(12) 45p.

SUMMARY

A three-dimensional steady state mathematical model of a cable used to suspend a sonar body from a helicopter is derived. Results are presented in dimensionless form for a length of cable totally immersed in any Newtonian fluid, and may therefore be applied to a number of practical problems. Various approximations are made in order to obtain analytical solutions. The suitability of the approximations is investigated by comparing solutions of the general and approximate equations for a uniform fluid velocity. In general, where maximum angular deviations from the vertical are small, agreement is observed to be very good. Two-dimensional 'power' and 'log' laws are assumed for the wind above the sea, and a three-dimensional Ekman spiral is assumed for the sea current. For these non-uniform fluid velocities, the concept of an 'equivalent mean fluid velocity' is used to simplify greatly the presentation of results.

POSTAL ADDRESS: Chief Superintendent, Aeronautical Research Laboratories,
Box 4331, P.O., Melbourne, Victoria, 3001, Australia.

CONTENTS

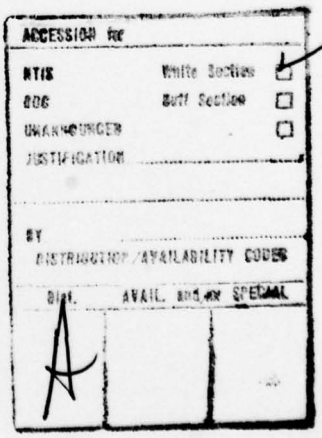

1. INTRODUCTION

For the underwater detection of submarines, helicopters commonly use a sonar body which is lowered by cable into the water. For efficient operation of the system, it is generally important for the sonar body to remain as close to the vertical as possible while submerged. For a calm sea with little or no wind, this is achieved by manoeuvring the helicopter, either manually or automatically via the helicopter control systems, in such a way that the cable deviations (in pitch and roll) from the vertical at the suspension point are kept close to zero. For the case of a steady non-zero wind, resulting cable bow requires one or both of these angular deviations to be kept constant at non-zero values. A mathematical model of the cable and sonar body enables these angles, which are referred to as "offset cable angle corrections", to be estimated and allows an investigation of the behaviour of the system under certain conditions. While hovering above the sea, the helicopter normally heads into wind and both speed of helicopter relative to ground and wind speed relative to helicopter are usually given by the helicopter instrumentation. It is assumed therefore that these quantities are given and that no further data about the air and sea environment are measured or known. A mathematical representation of the air and sea must therefore be assumed in order to calculate the fluid drag force on the cable and sonar body.

A three-dimensional time-dependent model in which the cable is represented by a number of rigid links is described in Reference 1. However, it is sufficient, and considerably more convenient, to consider a steady state model to investigate much of the behaviour of the system. This applies particularly to the problem of calculating the offset cable angle corrections, which need to be assumed invariant with time. The treatment ignores the sea waves which would cause non-steady effects, including cable oscillation. Steady state solutions have been presented by other authors,[2,3,4] but are restricted to two-dimensional motion in a uniform flowfield. These restrictions are removed in this document. Results are presented in dimensionless form for a length of cable totally immersed in any Newtonian fluid, and may therefore be applied to a number of cable problems.

The general equilibrium equations are first derived in Section 2. Solutions to these equations giving cable orientation at the top end of the cable are then presented in Section 3. The equations are solved numerically using the Runge-Kutta second order method for the general case and analytically for the two-dimensional case with uniform fluid velocity.† Various approximations are then made which allow an analytical solution for the three-dimensional case. The suitability of the approximations is shown by parameter studies in which uniform fluid velocity solutions of the general and approximate equations are compared.

In Section 4, it is shown that a non-uniform fluid velocity may be replaced by an "equivalent mean fluid velocity", thus greatly simplifying the presentation of results. This concept is also of use in developing a mathematical model for a flight simulator, where it is important to simplify the representation of the environment as much as possible. Equivalent mean fluid velocities are then presented for typical wind and sea velocity profiles. These include two-dimensional "power" and "log" laws for the wind above the sea, and a three-dimensional Ekman spiral for the sea current. Comparisons, similar to those for the uniform fluid velocity case, are made between solutions of the general and approximate equations. Finally, an example is given that is typical of a sonar body suspended from a helicopter.

2. MATHEMATICAL MODEL

2.1 Approach

In order to investigate the behaviour of a cable used to suspend a sonar body from a helicopter, the following steady state mathematical model is formulated. Given the tension and

† Derivations of analytical solutions are given in Reference 2 but are repeated here for completeness of presentation in the notation of this document.

angular orientation of the cable at the attached body, the angular orientation of the cable at the helicopter is required for any given steady state relative motion between the helicopter and the air and sea. When the body is submerged, a solution is first obtained for the length of cable also submerged. This solution then provides the necessary boundary conditions for the solution for the length of cable above the sea.

Consider then a length of cable, totally immersed in a Newtonian fluid, with the fluid moving horizontally. It is assumed that the only forces acting on the cable are the tension force, effective gravitational force (i.e. including buoyancy effect), and fluid drag force normal to the cable. Effects of cable twist, skin friction, induced mass, and elasticity of the cable are not considered here. The tension force and angular orientation at P_1, the lower end of the cable length, are assumed given. For steady state motion, the angular orientation at P_0, the upper end of the cable length, is required.

2.2 Axes Systems

It is convenient to define the following four right-handed orthogonal axes systems:

(a) *Cable axes—xyz*

The origin is at P_0. The z axis is vertical and positive downwards. The x axis is horizontal and lies in the fuselage longitudinal plane of symmetry (positive forward). The y axis forms a right-handed orthogonal axes system.

(b) *Earth axes—$x_E y_E z_E$*

The earth axes coincide with the cable axes at any arbitrarily chosen instant of time.

(c) *Cable element axes—$x_s y_s z_s$*

Cable element axes are defined for each element of length δs of cable. The origin P is at a distance s along the cable from P_0 and has coordinates (x, y, z) in cable axes. The z_s axis is tangential to the cable at P and is positive in the normally downward direction. The x_s axis is normal to the z_s axis and lies in the vertical plane containing the z_s axis. The y_s axis forms a right-handed orthogonal axes system.

(d) *Intermediate rotation axes—$x'y'z'$*

Intermediate axes are obtained when rotating xyz axes to give $x_s y_s z_s$ axes (see below and refer to Figure 1).

Earth axes serve only to define the separate cable and fluid motions with respect to earth. For the motion of fluid relative to the cable required in the analysis below, cable axes are used. It should be noted though that because of the invariance with time of the cable and fluid motion, the x_E, y_E, and z_E directions are always the same as the respective x, y, and z directions.

Angular orientation of the cable element axes relative to the cable axes is expressed in terms of the conventional Euler angles used in aircraft aerodynamics where the order of rotation is yaw, pitch, and roll. However, because effects of cable twist are ignored, only two angles are required to define the orientation. In general, for the conditions assumed, yaw angle will vary between $-180°$ and $180°$, whereas the magnitude of pitch and roll angle will always be less than $90°$. Hence, by choosing to use pitch and roll angle, singularities that occur at angles of $\pm 90°$ are avoided. Following parallel translation of the cable axes such that their origin coincides with the origin of the cable element axes, Figure 1 shows the appropriate angular rotations. The xyz axes are first rotated through an angle θ about the y axis to give intermediate axes, $x'y'z'$. These axes are then rotated through an angle ϕ about the x' axis to give the cable element axes, $x_s y_s z_s$.

Although the pitch and roll angles, θ and ϕ, are mostly used in the following analysis, in some instances it is convenient to use angles obtained by a rotation in yaw, χ, followed by pitch, γ. The angles may be related to θ and ϕ by considering the direction cosines of the cable element axes with respect to the cable axes. The direction cosines are given by Duncan[5] as

$$\cos \alpha = dx/ds = \sin \theta \cos \phi \tag{1a}$$

$$\cos \beta = dy/ds = -\sin \phi \tag{1b}$$

$$\cos \gamma = dz/ds = \cos \theta \cos \phi \tag{1c}$$

where the pitch angle γ is given directly by Equation (1c), and the yaw angle χ is given by

$$\tan \chi = \cos \beta / \cos \alpha = -\operatorname{cosec} \theta \tan \phi \tag{2}$$

2.3 Matrix Transformations for Rotations Through Pitch and Roll Angles

To resolve the various forces into the one axes system, it is convenient to first present some useful matrix transformations.[6]

Rotation of a vector through angles θ and ϕ is performed by premultiplying the vector by matrices Θ and Φ respectively, where

$$\Theta = \begin{bmatrix} \cos\theta & 0 & -\sin\theta \\ 0 & 1 & 0 \\ \sin\theta & 0 & \cos\theta \end{bmatrix}, \quad \Phi = \begin{bmatrix} 1 & 0 & 0 \\ 0 & \cos\phi & \sin\phi \\ 0 & -\sin\phi & \cos\phi \end{bmatrix} \tag{3}$$

and the respective matrix inverses are

$$\Theta^{-1} = \begin{bmatrix} \cos\theta & 0 & \sin\theta \\ 0 & 1 & 0 \\ -\sin\theta & 0 & \cos\theta \end{bmatrix}, \quad \Phi^{-1} = \begin{bmatrix} 1 & 0 & 0 \\ 0 & \cos\phi & -\sin\phi \\ 0 & \sin\phi & \cos\phi \end{bmatrix} \tag{4}$$

The matrix transformation obtained by rotating through an angle θ followed by a rotation through ϕ is

$$\Phi\,\Theta = \begin{bmatrix} \cos\theta & 0 & -\sin\theta \\ \sin\theta\sin\phi & \cos\phi & \cos\theta\sin\phi \\ \sin\theta\cos\phi & -\sin\phi & \cos\theta\cos\phi \end{bmatrix} \tag{5}$$

with the inverse given by

$$[\Phi\,\Theta]^{-1} = \Theta^{-1}\,\Phi^{-1} = \begin{bmatrix} \cos\theta & \sin\theta\sin\phi & \sin\theta\cos\phi \\ 0 & \cos\phi & -\sin\phi \\ -\sin\theta & \cos\theta\sin\phi & \cos\theta\cos\phi \end{bmatrix} \tag{6}$$

Inspection shows that the rotation matrices have the property that their inverses are the same as their transposes.

2.4 Velocity of Cable Relative to Fluid

It is assumed that both the cable and fluid may move in any horizontal direction defined by the angle between the velocity direction and the x direction, the angle increasing positively in the usual right-handed sense. The magnitude of the cable and fluid velocities relative to earth are defined as $u_H{}^*$ and $u_F{}^*$ respectively, with corresponding directions ψ_H and ψ_F. The quantities $u_H{}^*$ and ψ_H are assumed uniform, and $u_F{}^*$ and ψ_F are assumed to be known functions of z. The magnitude and direction of the velocity of the fluid relative to the cable are defined as u^* and ψ, with x, y, and z components given by the vector

$$\begin{bmatrix} u \\ v \\ w \end{bmatrix} = \begin{bmatrix} u_F \\ v_F \\ 0 \end{bmatrix} - \begin{bmatrix} u_H \\ v_H \\ 0 \end{bmatrix} \tag{7}$$

where

$$\begin{aligned} u_F &= u_F{}^* \cos\psi_F, & v_F &= u_F{}^* \sin\psi_F \\ u_H &= u_H{}^* \cos\psi_H, & v_H &= u_H{}^* \sin\psi_H \\ u &= u^* \cos\psi, & v &= u^* \sin\psi \end{aligned}$$

On resolving in cable element axes, the relative fluid velocity vector is given by

$$\begin{bmatrix} u_s \\ v_s \\ w_s \end{bmatrix} = \Phi\,\Theta \begin{bmatrix} u \\ v \\ 0 \end{bmatrix} = \begin{bmatrix} u\cos\theta \\ u\sin\theta\sin\phi + v\cos\phi \\ u\sin\theta\cos\phi - v\sin\phi \end{bmatrix} \tag{8}$$

The velocity component w_s is not required since skin friction is ignored. The velocity magnitude and direction, $u_s{}^*$ and ψ_s, in cable element axes, are defined by

$$u_s{}^* = (u_s{}^2 + v_s{}^2)^{\frac{1}{2}} \tag{9a}$$

$$\psi_s = \arctan\,(v_s/u_s) \tag{9b}$$

2.5 Equilibrium Equations

For a cable element of length δs at P (see Figure 2), the gravitational, fluid, and tension forces acting on the element are first resolved in cable element axes. Since the relative motion is steady state, these forces are in equilibrium so that

$$\text{Tension Force} + \text{Fluid Force} + \text{Gravitational Force} = 0$$

which may be rewritten using corresponding vectors expressed in cable element axes as

$$\begin{bmatrix} T_x \\ T_y \\ T_z \end{bmatrix} + \begin{bmatrix} F_x \\ F_y \\ F_z \end{bmatrix} + \begin{bmatrix} G_x \\ G_y \\ G_z \end{bmatrix} = \begin{bmatrix} 0 \\ 0 \\ 0 \end{bmatrix} \tag{10}$$

The gravitational and fluid forces are assumed to act at P, the upper end of the cable element. The gravitational force vector is given by

$$\begin{bmatrix} G_x \\ G_y \\ G_z \end{bmatrix} = \Phi\,\Theta \begin{bmatrix} 0 \\ 0 \\ mg\,\delta s \end{bmatrix} = mg\,\delta s \begin{bmatrix} -\sin\theta \\ \cos\theta \sin\phi \\ \cos\theta \cos\phi \end{bmatrix} \tag{11}$$

where m is the effective cable mass per unit length (allowing for buoyancy effect) and g is the gravitational acceleration (along the z axis). The fluid force vector is given by

$$\begin{bmatrix} F_x \\ F_y \\ F_z \end{bmatrix} = k_c\,\delta s\,(u_s^*)^2 \begin{bmatrix} \cos\psi_s \\ \sin\psi_s \\ 0 \end{bmatrix} = k_c\,\delta s\,u_s^* \begin{bmatrix} u_s \\ v_s \\ 0 \end{bmatrix} \tag{12}$$

where

$$k_c = \tfrac{1}{2}\rho_F\,d_c\,C_D \tag{13}$$

and ρ_F is the fluid density, d_c is the cable diameter, and C_D is the drag coefficient of the cable in the lateral direction of flow.

Let the tension force at P acting on the upper end of the element be T (i.e. along z_s axis in negative direction). Then the tension force at the lower end is $T + \delta T$ with orientation relative to cable axes given by a rotation in pitch of $\theta + \delta\theta$ followed by a rotation in roll of $\phi + \delta\phi$. The resultant tension force vector, in cable element axes, acting on the element is then given by

$$\begin{bmatrix} T_x \\ T_y \\ T_z \end{bmatrix} = \Phi\,\Theta\,\Theta_t^{-1}\,\Phi_t^{-1} \begin{bmatrix} 0 \\ 0 \\ T + \delta T \end{bmatrix} - \begin{bmatrix} 0 \\ 0 \\ T \end{bmatrix} \tag{14}$$

where the matrices Θ_t and Φ_t are used to rotate a vector through angles $\theta + \delta\theta$ and $\phi + \delta\phi$ respectively, and are defined by substituting $\theta + \delta\theta$ for θ, and $\phi + \delta\phi$ for ϕ, in Equations (3). Similar substitution in Equation (6) defines $\Theta_t^{-1}\,\Phi_t^{-1}$. On neglecting second order and higher order differences so that

$$\sin(\theta + \delta\theta) = \sin\theta + \delta\theta\cos\theta \tag{15a}$$

$$\cos(\theta + \delta\theta) = \cos\theta - \delta\theta\sin\theta \tag{15b}$$

with similar relations for $\sin(\phi + \delta\phi)$ and $\cos(\phi + \delta\phi)$, Equation (14) may be simplified to

$$\begin{bmatrix} T_x \\ T_y \\ T_z \end{bmatrix} = (T + \delta T) \begin{bmatrix} \delta\theta\cos\phi \\ -\delta\phi \\ 1 \end{bmatrix} - T \begin{bmatrix} 0 \\ 0 \\ 1 \end{bmatrix} = \begin{bmatrix} T\,\delta\theta\cos\phi \\ -T\,\delta\phi \\ \delta T \end{bmatrix} \tag{16}$$

On substituting Equations (11), (12), and (16) in Equation (10),

$$\begin{bmatrix} T\,\delta\theta\cos\phi \\ -T\,\delta\phi \\ \delta T \end{bmatrix} + k_c\,\delta s\,u_s^* \begin{bmatrix} u_s \\ v_s \\ 0 \end{bmatrix} + mg\,\delta s \begin{bmatrix} -\sin\theta \\ \cos\theta\sin\phi \\ \cos\theta\cos\phi \end{bmatrix} = \begin{bmatrix} 0 \\ 0 \\ 0 \end{bmatrix} \tag{17}$$

In the limit, as δs tends to zero, Equation (17) may be written in differential form as

$$T \cos \phi \frac{d\theta}{ds} = mg \sin \theta - k_c u_s^* u_s \tag{18a}$$

$$T \frac{d\phi}{ds} = mg \cos \theta \sin \phi + k_c u_s^* v_s \tag{18b}$$

$$\frac{dT}{ds} = - mg \cos \theta \cos \phi \tag{18c}$$

Using Equation (1c), where $dz/ds = \cos \theta \cos \phi$, the above equations may be transformed to

$$\frac{d\theta}{dz} = \frac{mg \sin \theta - k_c u_s^* u_s}{T \cos \theta \cos^2 \phi} \tag{19a}$$

$$\frac{d\phi}{dz} = \frac{mg \cos \theta \sin \phi + k_c u_s^* v_s}{T \cos \theta \cos \phi} \tag{19b}$$

$$\frac{dT}{dz} = - mg \tag{19c}$$

which are the basic equilibrium equations, in differential form, used here.

3. SOLUTION OF EQUILIPRIUM EQUATIONS

In their most general form, Equations (19a, b, c) can only be solved numerically. However, analytical solutions are possible given further assumptions or approximations. Solutions of both the general and approximate equations, which are termed "general" and "approximate" solutions respectively, are given below. As a convenient reference, a classification of these solutions is given in Table 1.

TABLE 1
Classification of Types of Solution of Equilibrium Equations

Solution type		Method of solution
1. General	(i) 2- or 3-D variable fluid velocity	Numerical solution of Equations (22a, b) using Runge-Kutta 2nd order method
	(ii) Restricted to 2-D uniform fluid velocity	Analytical solution given by Equation (26)
2. Approx.*	(i) 2- or 3-D variable fluid velocity	Approximate solution given by Equations (33a, b) requiring evaluations of integral by Simpson's formula
	(ii) Restricted to uniform fluid velocity†	Analytical solution given by Equations (34a, b)

3.1 General Equations

To obtain a solution of Equations (19a, b, c), Equation (19c) is first integrated between P and P_1 (where $z = z_1$ and $T = T_1$), to give

$$\int_T^{T_1} dT = - mg \int_z^{z_1} dz \tag{20}$$

* Approximations are (a) cable mass concentrated at attached body and (b) small angle approximations.

† Inciuding non-uniform fluid velocity if equivalent mean fluid velocity components are obtained analytically.

which results in

$$T = T_1 - mg\,(z - z_1) \tag{21}$$

The dimensionless quantities $\mu = mgz_1/T_1$, $X = x/z_1$, $Y = y/z_1$, $Z = z/z_1$, $S = s/z_1$, and $U^* = (k_c\, z_1/T_1)^{\frac{1}{2}}u^*$ (similarly for all velocities, e.g. $V = (k_c\, z_1/T_1)^{\frac{1}{2}}v$) are now introduced with the subscripts already used retaining their meaning. On substituting for T from Equation (21), Equations (19*a*, *b*) may be written in terms of the dimensionless quantities as

$$\frac{d\theta}{dZ} = \frac{\mu \sin\theta - U_s^*\, U_s}{[1 - \mu(Z - 1)] \cos\theta \cos^2\phi} \tag{22a}$$

$$\frac{d\phi}{dZ} = \frac{\mu \cos\theta \sin\phi + U_s^*\, V_s}{[1 - \mu(Z - 1)] \cos\theta \cos\phi} \tag{22b}$$

Given $\theta = \theta_1$ and $\phi = \phi_1$ at P_1, the above pair of simultaneous linear differential equations must be solved in order to obtain the angles $\theta = \theta_0$ and $\phi = \phi_0$ at P_0, where $Z = 0$. Knowing the angles θ and ϕ, the cable shape can readily be evaluated by numerical integration of Equations (1*a*, *b*, *c*) (see Part 1 of Appendix A).

3.1.1 Numerical Solution for General Case

For the general case, Equations (22*a*, *b*) are solved numerically using a Runge-Kutta second order method. For the special case described in Section 3.1.2, i.e. two-dimensional case with a uniform fluid velocity, an analytical solution is possible. A direct check on the accuracy of the numerical method may therefore be made for this case. This was done to first check the method and then to obtain a suitable integration interval to be used for more general conditions where an analytical solution is not possible. When used for each different type of condition, further checks were made in the usual way by comparing solutions for varying integration intervals. It was found that an integration interval in Z of 0·02 gave sufficient plotting accuracy for the curves presented in the figures.

3.1.2 Analytical Solution for Special Case

For the special case of a two-dimensional solution for a uniform fluid velocity, an analytical solution of Equations (22*a*, *b*) is possible.† A two-dimensional solution in any arbitrarily rotated vertical plane is most directly given by using, instead of θ and ϕ, the variables χ and γ, where $|\chi|$ is constant and $\gamma \geqslant 0$. However, because of possible sign changes in χ, it is more convenient to consider the xz plane, using θ and ϕ, where θ may be positive or negative, and $\phi = 0$. For a subsequent rotation of the vertical plane, γ is then given by the value of $|\theta|$ previously calculated for the xz plane.

Setting $\phi = 0$, $V = 0$, and $U = U_0$, then $U_s^* = |U_s|$, $U_s = U_0 \cos\theta$, and Equations (22*a*, *b*) reduce to the single equation

$$\frac{d\theta}{dZ} = \frac{\mu \sin\theta - U_0\,|U_0| \cos^2\theta}{[1 - \mu(Z - 1)] \cos\theta} \tag{23}$$

On integrating Equation (23) between P_0 and P,

$$\int_Z^1 \frac{dZ}{[1 - \mu(Z - 1)]} = \int_\theta^{\theta_1} \frac{\cos\theta}{[\mu \sin\theta - U_0\,|U_0| \cos^2\theta]}\, d\theta \tag{24}$$

Putting $t = \sin\theta$, $a = \mu/[U_0\,|U_0|]$, $q = (1 + 4/a^2)^{\frac{1}{2}}$, and $b = 1 + \mu(1 - Z)$, Equation (24) may be written as

† Refer to footnote on page 1.

$$\ln b = a \int_{t}^{t_1} \frac{dt}{(t^2 + at - 1)}$$

$$= \frac{1}{q} \left[\ln \left\{ \frac{[2t - a(q-1)]}{[2t + a(q+1)]} \right\} \right]_{t}^{t_1}$$

$$= \frac{1}{q} \ln \left\{ \frac{[2t_1 - a(q-1)]\ [2t + a(q+1)]}{[2t_1 + a(q+1)]\ [2t - a(q-1)]} \right\} \tag{25}$$

which gives

$$\sin\theta = \frac{2(b^q - 1) + a[b^q(q-1) + (q+1)] \sin\theta_1}{a[(q-1) + b^q(q+1)] + 2(b^q - 1) \sin\theta_1} \tag{26}$$

As a special case, when $\theta_1 = 0$, Equation (26) becomes

$$\sin\theta = \frac{2(b^q - 1)}{a[(q-1) + b^q(q+1)]} \tag{27}$$

The angle $\theta = \theta_0$ at P_0 is given by setting $Z = 0$ (i.e. $b = 1 + \mu$).

3.2 Approximate Equations

To obtain an analytical three-dimensional solution, the following approximations are found to be convenient:

(*a*) the "effective" cable mass is considered to be concentrated at the attached body;

(*b*) small angle approximations for θ and ϕ are assumed (i.e. $\sin\theta \approx \theta$, $\cos\theta \approx 1$, and similarly for ϕ).

For approximation (*a*) to be valid, either the ratio of cable mass to body mass, or the angles θ and ϕ, must be small.

Approximation (*a*) is achieved by setting $m = 0$ in Equations (19*a*, *b*, *c*) to give

$$\frac{d\theta}{dz} = \frac{-k_c u_s^* u_s}{T \cos\theta \cos^2\phi} \tag{28a}$$

$$\frac{d\phi}{dz} = \frac{k_c u_s^* v_s}{T \cos\theta \cos\phi} \tag{28b}$$

$$\frac{dT}{dz} = 0 \tag{28c}$$

where the tension T_1 at P_1 is now replaced by $T_1 + mgz_1$. From Equation (28*c*), the tension along the cable is seen to be constant and is given by

$$T = T_1 + mgz_1 = T_1(1 + \mu) \tag{29}$$

Substituting for T from Equation (29), Equations (28*a*, *b*) may be written in dimensionless form as

$$\frac{d\theta}{dZ} = \frac{-U_s^* U_s}{(1+\mu) \cos\theta \cos^2\phi} \tag{30a}$$

$$\frac{d\phi}{dZ} = \frac{U_s^* V_s}{(1+\mu) \cos\theta \cos\phi} \tag{30b}$$

Using approximation (*b*), then from Equation (8), $U_s \approx U$, $V_s \approx V$, and $U_s^* \approx U^*$, and Equations (30*a*, *b*) may be written as

$$\frac{d\theta}{dZ} = \frac{-U^* U}{(1+\mu)} \tag{31a}$$

$$\frac{d\phi}{dZ} = \frac{U^* V}{(1+\mu)} \tag{31b}$$

In Equations (31*a*, *b*) and below, the variables U and V may be alternatively expressed in terms of U^* and ψ using the relations

$$U = U^* \cos\psi \tag{32a}$$

$$V = U^* \sin\psi \tag{32b}$$

On integrating Equations (31*a*, *b*) between P and P_1,

$$\theta = \theta_1 + \frac{1}{(1+\mu)} \int_z^1 U^* U \, dZ \tag{33a}$$

$$\phi = \phi_1 - \frac{1}{(1+\mu)} \int_z^1 U^* V \, dZ \tag{33b}$$

where the angles $\theta = \theta_0$ and $\phi = \phi_0$ at P_0 are given by setting $Z = 0$. Equations (33*a*, *b*) provide an analytical three-dimensional solution provided a suitable fluid velocity function is chosen such that the integrations can be performed analytically. The cable shape may readily be obtained using the above small angle approximations (see Part 2 of Appendix A).

3.3 Comparison Between Uniform Fluid Velocity Solutions of General and Approximate Equations

For a uniform fluid velocity (i.e. $U^* = U_0^*$, $U = U_0$, $V = V_0$, and $\psi = \psi_0$) the integrations in Equations (33*a*, *b*) can be performed analytically to give

$$\theta = \theta_1 + U_0^* U_0 (1 - Z)/(1 + \mu) \tag{34a}$$

$$\phi = \phi_1 - U_0^* V_0 (1 - Z)/(1 + \mu) \tag{34b}$$

or, using Equations (32*a*, *b*),

$$\theta = \theta_1 + (U_0^*)^2 \cos\psi_0 (1 - Z)/(1 + \mu) \tag{35a}$$

$$\phi = \phi_1 - (U_0^*)^2 \sin\psi_0 (1 - Z)/(1 + \mu) \tag{35b}$$

The validity of the "approximate" solutions is discussed below by comparing them with appropriate "general" solutions for both two-dimensional and three-dimensional cases.

3.3.1 Two-dimensional Solution

For the two-dimensional case with uniform fluid velocity, the "general" solution is given analytically by Equation (26). To obtain a corresponding "approximate" solution, set $U_0^* = |U_0|$ in Equation (34*a*). Hence, the "approximate" solution in the xz plane is

$$\theta = \theta_1 + U_0 |U_0| (1 - Z)/(1 + \mu) \tag{36}$$

At $Z = 0$, comparisons between this solution and the "general" solution are given in Figures 3 to 5 for appropriate values of the parameters μ, θ_1, and U_0, where $U_0 > 0$. For $U_0 < 0$, symmetry considerations readily provide appropriate solutions, i.e. sign changes in U_0 and θ_1 result in a sign change in θ_0. When considering the length of cable in air, negative U_0 is the more usual case since the helicopter normally heads into wind. A few results, which show cable shapes for various parameter values, are presented in Figure 6. It can be seen in Figures 3 to 6 that agreement is good where maximum angular deviations of the cable from the vertical are small (usually for small values of the parameters μ, θ_1, and U_0). As one would expect when these deviations become large, approximation (*b*), and hence approximation (*a*) when μ is not small, become increasingly less valid, resulting in poor agreement.

3.3.2 Three-dimensional Solution

In presenting three-dimensional solutions, it is convenient to specify the boundary conditions at P_1 in terms of χ_1 and γ_1, instead of θ_1 and ϕ_1. From Equations (1*c*) and (2), θ and ϕ are given directly from the relations

$$\tan\theta = \tan\gamma\cos\chi \tag{37a}$$

$$\sin\phi = -\sin\gamma\sin\chi \tag{37b}$$

so that θ_1 and ϕ_1 may be readily obtained. At $Z = 0$, Figures 7 to 9 show comparisons between three-dimensional solutions of angular orientation in pitch and roll obtained using the "approximate" solutions given by Equations (35*a*, *b*) and the "general" solution of Equations (22*a*, *b*) for appropriate values of the parameters μ, χ_1, γ_1, $U_0{}^*$, and ψ_0. For three specific cases, corresponding comparisons between cable shapes are illustrated in Figure 10. In these figures, where an arbitrary choice of ψ_0 is required, the value $\pm 180°$ is chosen; as previously stated, this corresponds to the usual case for the length of cable in air. As found with the two-dimensional case, where maximum angular deviations from the vertical are small (usually for small values of the parameters μ, γ_1, and $U_0{}^*$), agreement is observed to be good; large deviations result in poor agreement.

4. SOLUTIONS FOR TYPICAL WIND PROFILES AND SEA CURRENTS

For the case of a non-uniform fluid velocity, it is convenient to obtain, as a first step, "equivalent values" of the mean fluid velocity components U_F and V_F. They are defined to be those values which give the same solution of Equations (33*a*, *b*) at $Z = 0$ as obtained when the actual non-uniform values are used. This requires

$$\langle U^*\rangle\langle U\rangle = \int_0^1 U^*\,U\,dZ \tag{38a}$$

$$\langle U^*\rangle\langle V\rangle = \int_0^1 U^*\,V\,dZ \tag{38b}$$

where all variables enclosed by "$\langle$" and "$\rangle$" are mean values. For any non-uniform velocity, once these equivalent values are calculated, solutions giving angular orientation may be readily obtained using the uniform velocity results of Section 3.3. This procedure greatly simplifies the *presentation of results.*

At this stage, non-dimensional velocities are scaled by $U_{F0}{}^*$ (assumed non-zero), the value of $U_F{}^*$ at P_0, to give $\omega = U_F{}^*/U_{F0}{}^*$, $\lambda = U_H{}^*/U_{F0}{}^*$, and $\sigma = U^*/U_{F0}{}^*$ with x and y components defined as

$$\omega_x = \omega\cos\psi_F = U_F/U_{F0}{}^*, \qquad \omega_y = \omega\sin\psi_F = V_F/U_{F0}{}^*$$

$$\lambda_x = \lambda\cos\psi_H = U_H/U_{F0}{}^*, \qquad \lambda_y = \lambda\sin\psi_H = V_H/U_{F0}{}^*$$

$$\sigma_x = \sigma\cos\psi = U/U_{F0}{}^*, \qquad \sigma_y = \sigma\sin\psi = V/U_{F0}{}^*$$

Assuming the scaled non-dimensional fluid velocity components ω_x and ω_y are known functions of Z, equivalent mean values $\langle\omega_x\rangle$ and $\langle\omega_y\rangle$ are now derived. Corresponding non-scaled values $\langle U_F\rangle$ and $\langle V_F\rangle$ may be obtained by multiplying by $U_{F0}{}^*$. From Equations (7) and (32*a*, *b*), the variables in Equations (38*a*, *b*) may be expressed in terms of the above scaled velocity components as

$$U = U_F - U_H = U_{F0}{}^*\,\sigma_x \tag{39a}$$

$$V = V_F - V_H = U_{F0}{}^*\,\sigma_y \tag{39b}$$

$$U^* = (U^2 + V^2)^{\frac{1}{2}} = |U_{F0}{}^*|\,(\sigma_x{}^2 + \sigma_y{}^2)^{\frac{1}{2}} \tag{39c}$$

$$\langle U\rangle = U_{F0}{}^*\,\langle\sigma_x\rangle \tag{40a}$$

$$\langle V\rangle = U_{F0}{}^*\,\langle\sigma_y\rangle \tag{40b}$$

$$\langle U^*\rangle = |U_{F0}{}^*|\,(\langle\sigma_x\rangle^2 + \langle\sigma_y\rangle^2)^{\frac{1}{2}} \tag{40c}$$

where $\langle\sigma_x\rangle = \langle\omega_x\rangle - \lambda_x$ and $\langle\sigma_y\rangle = \langle\omega_y\rangle - \lambda_y$.

Substituting Equations (39*a*, *b*, c) and (40*a*, *b*, *c*) in Equations (38*a*, *b*),

$$(\langle\sigma_x\rangle^2 + \langle\sigma_y\rangle^2)^{\frac{1}{2}}\,\langle\sigma_x\rangle = \beta_x \tag{41a}$$

$$(\langle\sigma_x\rangle^2 + \langle\sigma_y\rangle^2)^{\frac{1}{2}}\,\langle\sigma_y\rangle = \beta_y \tag{41b}$$

where

$$\beta_x = \int_0^1 U^* \, U \, dZ = \int_0^1 (\sigma_x{}^2 + \sigma_y{}^2)^{\frac{1}{2}} \, \sigma_x \, dZ$$

$$\beta_y = \int_0^1 U^* \, V \, dZ = \int_0^1 (\sigma_x{}^2 + \sigma_y{}^2)^{\frac{1}{2}} \, \sigma_y \, dZ$$

Equations (41*a*, *b*) may be solved for $\langle \omega_x \rangle$ and $\langle \omega_y \rangle$ to give

$$\left.\begin{aligned} \langle \omega_x \rangle &= \lambda_x + \alpha_x \, |\beta_x| / \beta_x \qquad \text{for } \beta_x \neq 0 \\ &= \lambda_x \qquad\qquad\qquad\quad \text{for } \beta_x = 0 \end{aligned}\right\} \tag{42a}$$

$$\left.\begin{aligned} \langle \omega_y \rangle &= \lambda_y + \alpha_y \, |\beta_y| / \beta_y \qquad \text{for } \beta_y \neq 0 \\ &= \lambda_y \qquad\qquad\qquad\quad \text{for } \beta_y = 0 \end{aligned}\right\} \tag{42b}$$

where

$$\alpha_x = \{|\beta_x| \, (1 + \beta_y{}^2/\beta_x{}^2)^{-\frac{1}{2}}\}^{\frac{1}{2}}$$

$$\alpha_y = \{|\beta_y| \, (1 + \beta_x{}^2/\beta_y{}^2)^{-\frac{1}{2}}\}^{\frac{1}{2}}$$

When the velocity of the fluid relative to the cable is two-dimensional, in the *xz* plane, Equations (41*a*, *b*) reduce to

$$|\langle \sigma_x \rangle| \, \langle \sigma_x \rangle = \beta_x \tag{43}$$

where

$$\beta_x = \int_0^1 |\sigma_x| \, \sigma_x \, dZ$$

which gives

$$\left.\begin{aligned} \langle \omega_x \rangle &= \lambda_x + |\beta_x|^{3/2} / \beta_x \qquad \text{for } \beta_x \neq 0 \\ &= \lambda_x \qquad\qquad\qquad\quad \text{for } \beta_x = 0 \end{aligned}\right\} \tag{44}$$

When the velocity of the fluid relative to the cable is three-dimensional, it is often convenient (see Section 4.1) to assume that, for the purpose of obtaining equivalent mean fluid velocity components $\langle \omega_x \rangle$ and $\langle \omega_y \rangle$, the *x* and *y* components of the relative fluid velocity can be treated independently. Then Equation (44) may be used to obtain $\langle \omega_x \rangle$, and a corresponding equation in the *y* direction may be used to obtain $\langle \omega_y \rangle$. Rewriting Equation (41*a*) in the form

$$|\langle \sigma_x \rangle| \, \sigma_x \, (1 + \langle \sigma_y \rangle^2 / \langle \sigma_x \rangle^2)^{\frac{1}{2}} = \int_0^1 |\sigma_x| \, \sigma_x \, (1 + \sigma_y{}^2/\sigma_x{}^2)^{\frac{1}{2}} \, dZ \tag{45}$$

it can be seen that by replacing σ_x and σ_y by $\langle \sigma_x \rangle$ and $\langle \sigma_y \rangle$ respectively only in the square root term of the integrand, this equation reduces to Equation (43). A similar result may be obtained from Equation (41*b*) for the *y* direction. If, over the range of integration, the variation of $(1 + \sigma_y{}^2/\sigma_x{}^2)^{\frac{1}{2}}$ is high, the approximation may be poor. It should be noted that this independent treatment of the velocity components (referred to as "independent velocity component assumption") is confined to the calculation of equivalent mean fluid velocity components; the uniform velocity three-dimensional results of Section 3.3.2 should be used to obtain angular deviations in pitch and roll.

In the following presentation of winds above the sea and ocean currents, subscripts *A* and *W* replace subscript *F* when the fluid is "air" and "water" respectively.

4.1 Winds Above the Sea

In representing the wind above the sea, it is assumed that wind direction does not vary with altitude and that the helicopter heads into wind. This results in $\psi_A = \psi_{A0} = \pm 180°$. Generally,

conditions above the sea are very difficult to predict and a number of different velocity functions are possible for various stability classifications.[7] The influence of the rotor downwash complicates the air flow even further. In view of these uncertainties, a mathematically complex function is not warranted. In fact, one may argue that a uniform velocity is sufficient, in which case the results already obtained in Section 3.3 may be used directly.

Two commonly used wind profiles, known as "power" and "log" laws, are assumed here and are defined below. The log law profile is as used for the neutral stability classification.[7] Each profile requires $\omega_x = 0$ at the sea surface and $\omega_x = -1$ at P_0. The dimensionless quantity H is defined as h/z_1, where h is the height of P_0 above the sea (i.e. hover height).

(*a*) Power Law

$$-\omega_x = (1 - Z/H)^{1/n} \tag{46}$$

where n is a positive integer, commonly assumed to be six.

(*b*) Log Law

$$-\omega_x = ln\,\{c - (c-1)\,Z/H\}/ln\,c \tag{47}$$

where $c = 1 + h/h_0$ and h_0 is the surface roughness length (on p. 140 of Ref. 7, $h_0 = 2{\cdot}5 \times 10^{-4}$ m for calm sea, $h_0 = 4{\cdot}0 \times 10^{-5}$ m for rough sea).

The above two formulae give very similar wind profiles provided the appropriate values for n and c are chosen.

For the wind profiles, the velocity of the fluid relative to the cable is two-dimensional provided any helicopter motion is in the same direction as the wind (i.e. $\psi_H = 0$ or $\pm 180°$, or $\lambda_y = 0$); otherwise, the relative velocity is three-dimensional. Using the "equivalent mean fluid velocity" concept, for the two-dimensional case, $\langle\omega_y\rangle = 0$ and $\langle\omega_x\rangle$ is readily given by Equation (44). However, for the three-dimensional case, $\langle\omega_x\rangle$ and $\langle\omega_y\rangle$ should be recalculated for each value of λ_y. It is therefore convenient to use the independent velocity component assumption outlined in Section 4. Then, for a given value of λ_x, the values $\langle\omega_x\rangle$ and $\langle\omega_y\rangle$ remain unchanged for all values of λ_y. For the wind profiles assumed, using typical parameter values experienced, this approximation was generally found to be good when $|\lambda_y|$ was reasonably small (i.e. less than about $0{\cdot}5$). This is to be expected since, for small λ_y, $(1 + \sigma_y^2/\sigma_x^2)^{\frac{1}{2}}$, which equals $\{1 + \lambda_y^2/(\omega_x - \lambda_x)^2\}^{\frac{1}{2}}$, does not differ significantly from unity throughout most of the range of integration for both profiles.

Analytical solutions for $\langle\omega_x\rangle$ from Equation (44) are possible. However, they are given by lengthy formulae so that, except for special cases, results presented here are obtained by integrating numerically using Simpson's formula. For the special case when $\lambda_x = 0$ and $H = 1$, from Equation (44), $\langle\omega_x\rangle$ is given analytically for the power law by

$$-\langle\omega_x\rangle = \left[\int_0^1 (1 - Z)^{2/n}\,dZ\right]^{\frac{1}{2}} = \left[\frac{n}{2+n}\right]^{\frac{1}{2}} \tag{48}$$

and for the log law by

$$-\langle\omega_x\rangle = \left[\int_0^1 \frac{ln^2\,\{c - (c-1)\,Z\}}{ln^2\,c}\,\lambda Z\right]^{\frac{1}{2}} = \left[\frac{c}{c-1}\left(1 - \frac{2}{ln\,c}\right) + \frac{2}{ln^2\,c}\right]^{\frac{1}{2}} \tag{49}$$

Figure 11 shows both profiles for a range of parameter values n and c. Pairs of the parameters have been suitably chosen to give similar profiles when each parameter is used in the appropriate law. At $\lambda_x = 0$ and for a number of values of $1/H$, points are shown on the curves at which $\langle\omega_x\rangle = \omega_x$. Using the same parameter values, Figure 12 shows the variation of $\langle\omega_x\rangle$ with λ_x at $H = 1$. The sudden change in $\langle\omega_x\rangle$ observed for each curve is produced by the effect of a reversal in the fluid drag force along the cable, i.e. σ_x changes sign.

Figure 13 shows comparisons between two-dimensional "general" and "approximate" solutions for θ_0 with the power law wind profile used. The former solution is obtained from Equation (22*a*) with $\phi = 0$ and $V = 0$, and the latter is given by Equation (36) with the equivalent mean fluid velocity used. As with the uniform velocity solutions, agreement is observed to be poor where large angular deviations from the vertical are experienced. Results for the log law were found to be very similar.

4.2 Sea Currents

Like winds above the sea, sea currents are extremely difficult to predict.[8] One may well similarly argue that any function, other than a uniform one, is not warranted, in which case results obtained in Section 3.3 may again be used directly. However, for a non-uniform velocity, the classical Ekman spiral[8] provides a mathematically convenient function that is fairly realistic for deep water, i.e. particularly for oceans. The dimensionless quantity D is defined as d/z_1, where d is the depth of frictional resistance. The magnitude and direction of the spiral is then defined for the southern hemisphere† and with $\psi_A = \pm 180°$ by

$$\omega = e^{-\pi Z/D} \tag{50a}$$

$$\psi_W = 3\pi/4 - \pi Z/D \tag{50b}$$

where ψ_W is in radians. Equations (48*a*, *b*) may be expressed in component form as

$$\omega_x = \omega \cos \psi_W = e^{-\pi Z/D} \cos (3\pi/4 - \pi Z/D) \tag{51a}$$

$$\omega_y = \omega \sin \psi_W = e^{-\pi Z/D} \sin (3\pi/4 - \pi Z/D) \tag{51b}$$

The above function is illustrated in Figure 14. At the sea surface, the direction of the current is 45° to the left (right, in the northern hemisphere) of the wind direction. At the depth of friction, i.e. when $Z = D$, the water velocity is 0·043 times the surface velocity, i.e. $\omega = 0{\cdot}043$. The significance attached to the depth d is that below it, the velocity is considered negligible.

For the cable length above the sea, the velocity u_{A0} at P_0 is generally known from helicopter instrumentation. For the submerged cable length, the water velocity $u_{W0}{}^*$ at P_0, as well as the depth of frictional resistance, d, are not generally given by any instrumentation. However, empirical expressions for both $u_{W0}{}^*$ and d have been derived. From References 8 and 9 respectively,

$$d \approx 7{\cdot}6\, u_{A0}{}^* \operatorname{cosec}^{\frac{1}{2}} \phi_E \tag{52a}$$

$$u_{W0}{}^* \approx 0{\cdot}03\, u_{A0}{}^* \tag{52b}$$

where ϕ_E is the geographical latitude and d is in metres for $u_{A0}{}^*$ in metres per second. At $\phi_E = 35°$, Equation (52*a*) gives $d \approx 10\, u_{A0}{}^*$. The above references assume $u_{A0}{}^*$ is measured at an altitude of 15 m and 10 m respectively. For the assumed wind profiles, $u_{A0}{}^*$ does not vary significantly with altitude in the range expected for a hovering helicopter with a sonar body suspended by a cable, i.e. roughly 10 m to 30 m. Hence, adjustment to the above formulae is not warranted for changes in altitude within this range.

In Reference 8, at wind velocities below about 6 m/s, Equation (52*a*) is replaced by

$$d \approx 3{\cdot}67(u_{A0}{}^*)^{3/2} \operatorname{cosec}^{\frac{1}{2}} \phi_E \tag{52c}$$

which, at $\phi_E = 35°$, gives $d \approx 4{\cdot}8(u_{A0}{}^*)^{3/2}$. However, this further refinement is not considered necessary in view of the limited confidence in the model of the sea current. Because the angular deviation of the cable is roughly proportional to the square of the velocity (see Equation (36)), errors are minimized over a large range of velocity by choosing the empirical relation given by Equation (52*a*), which is more appropriate for higher velocities, Neither relation allows a meaningful estimate for d at the equator, i.e. at $\phi_E = 0$.

During normal sonar operation, it is generally desirable for the sonar body to reman vertical. For the mathematical model used here, this requires (for $\gamma_1 = 0$) the relative fluid velocity at the body to be zero, i.e. $\lambda_x = \omega_{x1}$ and $\lambda_y = \omega_{y1}$, where ω_{x1} and ω_{y1} are the values of ω_x and ω_y respectively at P_1. Equivalent mean fluid velocities, which are obtained by integrating numerically using Simpson's formula, are therefore presented assuming this condition.

In Figure 15, both the Ekman spiral and equivalent mean fluid velocity are shown in the xy plane as functions of Z/D and $1/D$ respectively. Equivalent mean fluid velocity values calculated using the independent velocity component assumption are compared with the values obtained without this assumption, i.e. using Equations (42*a*, *b*). Agreement is seen to be very good for the lower and upper range of values of $1/D$ shown. As explained in Section 4, regions of good agreement imply there is only small variation in the term $(1 + \sigma_y{}^2/\sigma_x{}^2)^{\frac{1}{2}}$ throughout the range of integration. The absolute error in the approximate values is given by the distance

† For the northern hemisphere, $\psi_W = -3\pi/4 + \pi Z/D$.

between points on the two mean velocity curves of Figure 15 which have the same value of $1/D$. This error is a maximum of 0·037 at $1/D \approx 1{\cdot}05$ and is about 0·01 at $1/D = 0{\cdot}6$ and 14. Although these errors are much larger than those generally experienced when considering winds above the sea, they may well be acceptable when viewed in relation to uncertainties already existing.

A three-dimensional "approximate" solution for θ_0 and ϕ_0 is obtained from Equations (34*a*, *b*) on using the equivalent mean velocity values shown in Figure 15. For appropriate values of the parameters μ and $U_{W0}{}^*$, solutions of angular orientation in pitch and roll are given in Figure 16 and are compared with solutions obtained using the "independent component" equivalent mean fluid velocities. Errors are seen to correspond to those observed in Figure 15. Results obtained from the "general" solution are not shown since they were found to agree very closely with the "approximate" solution results (i.e. full lines of Figure 16). Good agreement is to be expected because the angular deviations from the vertical are small.

4.3 Example of Sonar Body Suspended from a Helicopter

So far, solutions have been presented only for a length of cable totally immersed in a single Newtonian fluid. However, the main case of interest in this study is of a sonar body suspended from a helicopter. Here, the cable passes through two fluid layers (air and water) and the method of approach outlined in Section 2.1 should be used.† Using a power law for the wind above the sea, and an Ekman spiral for the sea current, an example is given below in which cable orientation and shape are determined.

Constants that are independent of the fluid are $g = 9{\cdot}81$ m/s^2, $d_c = 20$ mm, $C_D = 1{\cdot}2$, and $u_H{}^* = 0$.

The assumed conditions in air are $\rho_A = 1{\cdot}226$ kg/m^3, $mg = 6{\cdot}2$ N/m, $z_1 = h = 20$ m (i.e. $H = h/z_1 = 1$), $u_{A0}{}^* = 20$ m/s, $\psi_A = \pm 180°$, and $n = 6$ (for power law).

The assumed conditions in water are $\rho_W = 1023$ kg/m^3, $T_1 = 60$ N, $z_1 = 40$ m, $d = 10\, u_{A0}{}^* = 200$ m (i.e. $D = d/z_1 = 5$), $u_{W0}{}^* = 0{\cdot}03\, u_{A0}{}^* = 0{\cdot}6$ m/s, $\gamma_1 = 20°$, $\chi_1 = \psi_1 = (0{\cdot}75\pi - \pi/D)$ rad $= 99°$ (i.e. at attached body, cable is inclined in a vertical plane in the flow direction), and $mg = 3{\cdot}0$ N/m (obtained by subtracting the upthrust, $\rho_W g\,(\frac{1}{4}\pi d_c)^2$, from the value of mg in air).

In water, using Equation (21), $T_0 = T_1 + mgz_1 = 180$ N, which is equal to T_1 in air. The dimensionless quantities μ and $U_0{}^*$ are then calculated for both air and water and are given in Table 2 together with a summary of the parameter values required in the calculations.

On numerically solving the general equations, cable orientation and linear displacement coordinates are obtained. Table 3 presents these values at the sonar body, sea surface, and helicopter. All displacement coordinates are expressed in terms of dimensionless coordinates for the cable in air and should be multiplied by 20 to give displacement in metres. Figure 17 illustrates the cable shape together with the horizontal fluid velocity vectors. For each fluid, these vectors represent the scaled velocity ω, where $\omega_0 = 1$.

† The method could easily be extended to any number of fluid layers.

TABLE 2
Parameter Values that are Dependent on Fluid

Quantity	Value in water	Value in air
ρ_F	1023 kg/m^3	1·226 kg/m^3
T_1	60 N	180 N
mg	3·0 N/m	6·2 N/m
z_1	40 m	20 m
$u_{F0}{}^*$	0·6 m/s	20 m/s
$k_c = \frac{1}{2}\rho_F d_c C_D$	12·3 kg/m^2	0·0147 kg/m^2
$(k_c z_1/T_1)^{\frac{1}{2}}$	2·86 s/m	0·0404 s/m
$\mu = mgz_1/T_1$	2·0	0·69
$U_0{}^* = U_{F0}{}^* = (k_c z_1/T_1)^{\frac{1}{2}} u_{F0}{}^*$	1·72	0·81

TABLE 3
Orientation Angles and Displacement Coordinates

Quantity	Value at: (1) Sonar body	(2) Sea surface	(3) Helicopter
θ	−3·3°	−17·5°	−26·3°
ϕ	−19·7°	−29·0°	−14·5°
X	−0·681	−0·393	0
Y	1·311	0·404	0
Z	3	1	0

5. CONCLUDING REMARKS

A three-dimensional steady state mathematical model of a cable used to suspend a sonar body from a helicopter has been derived. The effect of the sea waves, which would make the problem unsteady, is neglected. Results are presented in dimensionless form for a length of cable totally immersed in a Newtonian fluid, and may therefore be applied to a number of practical problems.

In order to obtain analytical solutions giving cable orientation at its suspension point, it is assumed that the orientation angles are small and that the cable mass is concentrated at the attached body. Solutions of the general and approximate equations are obtained for the case when the fluid velocity is uniform. In general, for both two-dimensional and three-dimensional cases, where maximum angular deviations from the vertical are small, agreement between the "general" and "approximate" solutions is good; large deviations usually result in poor agreement.

The use of an equivalent mean fluid velocity to replace any non-uniform profile allows solutions to be readily obtained from the uniform velocity results presented in the figures. This enables a more compact presentation of results for the various non-uniform fluid velocity profiles used here. These non-uniform profiles include two-dimensional "power" and "log" laws for the wind above the sea, and a three-dimensional Ekman spiral for the sea current. The above concept would also be very useful for simplifying the representation of the environment in developing a mathematical model for a flight simulator. Comparisons between non-uniform fluid velocity solutions of the general and approximate equations result in similar conclusions to those found for the uniform fluid velocity case.

ACKNOWLEDGMENT

The author is indebted to Dr G. D. Mallinson for use of his graphics computer programs, which were used to obtain various views of three-dimensional images.

NOTATION

C_D	Drag coefficient of cable in the lateral direction of flow.
D	d/z_1
$\{F_x, F_y, F_z\}$	Fluid force vector
$\{G_x, G_y, G_z\}$	Gravitational force vector
H	h/z_1
P	Upper end of cable element
P_0	Upper end of cable length
P_1	Lower end of cable length
S	s/z_1
T	Tension force at P
$\{T_x, T_y, T_z\}$	Tension force vector
U^*	Non-dimensional velocity magnitude $(k_c z_1/T_1)^{\frac{1}{2}} u^*$
U, V	x, y components of U^*
X, Y, Z	$x/z_1, y/z_1, z/z_1$
a	$\mu/[U_0 \lvert U_0 \rvert]$
b	$1 + \mu(1 - Z)$
c	$1 + h/h_o$
d	Depth of frictional resistance
d_c	Cable diameter
g	Gravitational acceleration (along z_E axis)
h	Height of P_0 above the sea (i.e. hover height)
h_o	Surface roughness length
k_c	$\frac{1}{2}\rho_F d_c C_D$
m	Effective cable mass per unit length (allowing for buoyancy effect)
n	Positive integer
q	$(1 + 4/a^2)^{\frac{1}{2}}$
s	Distance of P from P_0 along cable
t	$\sin\theta$
u^*	Velocity of magnitude fluid relative to cable
u_F^*, u_H^*	Velocity magnitude of fluid, cable relative to earth
u, v, w	x, y, z components of velocity of fluid relative to cable
u_F, v_F	x, y components of fluid velocity in earth axes

u_H, v_H	x, y components of cable velocity in earth axes
xyz	Cable axes
$x'y'z'$	Intermediate rotation axes
$x_E y_E z_E$	Earth axes
$x_s y_s z_s$	Cable element axes
x, y, z	Linear displacement components of P in cable axes
Θ, Φ	Matrices representing rotations through θ, ϕ
Θ_t, Φ_t	Matrices representing rotations through $\theta + \delta\theta$, $\phi + \delta\phi$
α, β, γ	Direction cosine angles of cable element axes with respect to cable axes
α_x	$\{\|\beta_x\|(1 + \beta_y^2/\beta_x^2)^{-\frac{1}{2}}\}^{\frac{1}{2}}$
α_y	$\{\|\beta_y\|(1 + \beta_x^2/\beta_y^2)^{-\frac{1}{2}}\}^{\frac{1}{2}}$
β_x	$\int_0^1 U^* U \, dZ$
β_y	$\int_0^1 U^* V \, dZ$
δ	Denotes increment in quantity prefixed
θ, ϕ	Pitch, roll Euler angles when rotating xyz axes to $x_s y_s z_s$ axes (pitch followed by roll)
λ	U_H^*/U_{F0}^*
λ_x, λ_y	x, y components of λ
μ	mgz_1/T_1
ρ_F	Fluid density
σ	U^*/U_{F0}^*
σ_x, σ_y	x, y components of σ
ϕ_E	Geographical latitude
χ, γ	Yaw, pitch Euler angles when rotating xyz axes to $x_s y_s z_s$ axes (yaw followed by pitch)
ψ	Velocity direction of fluid relative to cable
ψ_F, ψ_H	Velocity direction of fluid, cable
ω	U_F^*/U_{F0}^*
ω_x, ω_y	x, y components of ω
$\{\}$	Used to write a column vector as a row vector
$\langle\rangle$	Enclosed quantity is a mean value

Subscripts:

A, W	Replaces subscript F when the fluid is air, water
s	Quantity is in cable element axes
0, 1	Value at P_0, P_1 (may follow other subscripts)

REFERENCES

1. Packer, T. J. "Wessex Helicopter/Sonar Dynamics Study. The Mathematical Model of the Sonar Cable and Transducer." WRE Report 951 (WR&D), May 1973.
2. Glauert, H. "The Form of a Heavy Flexible Cable Used for Towing a Heavy Body below an Aeroplane." Aeronautical Research Committee, R&M 1592, 1934.
3. Landweber, L. and Protter, M. H. "The Shape and Tension of a Light Flexible Cable in a Uniform Current." Journal of Applied Mechanics, Transactions of ASME, Vol. 14, 1947, pp. 121–126.
4. Genin, J. and Cannon, T. C. "Equilibrium Configuration and Tensions of a Flexible Cable in a Uniform Flowfield." Journal of Aircraft, Vol. 4, May–June 1967, pp. 200–202.
5. Duncan, W. J. "The Principles of the Control and Stability of Aircraft." Cambridge University Press, 1959, p. 79.
6. Etkin, B. "Dynamics of Atmospheric Flight." Wiley, New York, 1972, p. 117.
7. Roll, H. U. "Physics of the Marine Atmosphere." Academic Press, New York, 1965, ch. 4.
8. Sverdrup, H. U., Johnson, M. W., and Flemming, R. H. "The Oceans." Prentice Hall, New York, 1946, ch. 13.
9. Spillane, K. T. "Movement of Oil on the Sea Surface." Aust. Met. Mag., Vol. 19, No. 4, 1971, pp. 158–77.

APPENDIX A

Cable Shape from General and Approximate Equations

(1) *General Equations*

In dimensionless form, derivatives of the cable coordinates X, Y and cable length S with respect to Z are given from Equations (1*a*, *b*, *c*) by

$$dX/dZ = \tan\theta$$

$$dY/dZ = -\sec\theta\tan\phi$$

$$dS/dZ = \sec\theta\sec\phi$$

On integrating between P and P_1,

$$X_1 - X = \int_z^1 \tan\theta\, dZ$$

$$Y_1 - Y = -\int_z^1 \sec\theta\tan\phi\, dZ$$

$$S_1 - S = \int_z^1 \sec\theta\sec\phi\, dZ$$

The left-hand side of each of the above equations is first determined at all required equispaced values of Z by integrating numerically for Z decreasing from one to zero. At $Z = 0$, the variables X, Y, and S are zero so that X_1, Y_1 and S_1 are given directly. This enables X, Y, and S to be obtained for $0 < Z < 1$ from the previously calculated left-hand sides. The above integrals are calculated using Simpson's formula following each step of the numerical method used to obtain θ and ϕ. This procedure is particularly suited to the Runge-Kutta second order method used (see Section 3.1.1), since the mid-interval values required by Simpson's formula are directly provided by the Runge-Kutta method.

(2) *Approximate Equations*

For small angles, the above equations may be written as†

$$X_1 - X \approx \int_z^1 \theta\, dZ$$

$$Y_1 - Y \approx -\int_z^1 \phi\, dZ$$

$$S_1 - S \approx \int_z^1 [1 + \tfrac{1}{2}(\theta^2 + \phi^2)]\, dZ$$

† Second order terms in θ and ϕ are retained for the expression for $S_1 - S$; otherwise $S \approx Z$.

Generally, for a variable fluid velocity, the procedure for obtaining X, Y, and S is as described above in Part (1). For a uniform fluid velocity, or a non-uniform one if the equivalent mean fluid velocity components are obtained analytically, θ and ϕ are given analytically as linear functions of Z (see Equations (34*a*, *b*)). On substituting these functions, integrating analytically, and then using Equations (34*a*, *b*) to simplify the result, we have

$$X_1 - X = \tfrac{1}{2}(1 - Z)(\theta_1 + \theta)$$

$$Y_1 - Y = -\tfrac{1}{2}(1 - Z)(\phi_1 + \phi)$$

$$S_1 - S = (1 - Z)[1 + \tfrac{1}{6}(\theta_1^2 + \theta_1\theta + \theta^2 + \phi_1^2 + \phi_1\phi + \phi^2)]$$

The variables X, Y, and S can be obtained as before, but because θ_0 and ϕ_0 are given directly without any numerical integration, use can be made of these values at commencement of the calculations. At P_0, the variables X, Y, Z, and S are all zero; hence the values X_1, Y_1, and S_1 are given by

$$X_1 = \tfrac{1}{2}(\theta_1 + \theta_0)$$

$$Y_1 = -\tfrac{1}{2}(\phi_1 + \phi_0)$$

$$S_1 = 1 + \tfrac{1}{6}(\theta_1^2 + \theta_1\theta_0 + \theta_0^2 + \phi_1^2 + \phi_1\phi_0 + \phi_0^2)$$

Using the two above sets of equations together with Equations (34*a*, *b*), the variables X, Y, and S are given directly for any value of Z.

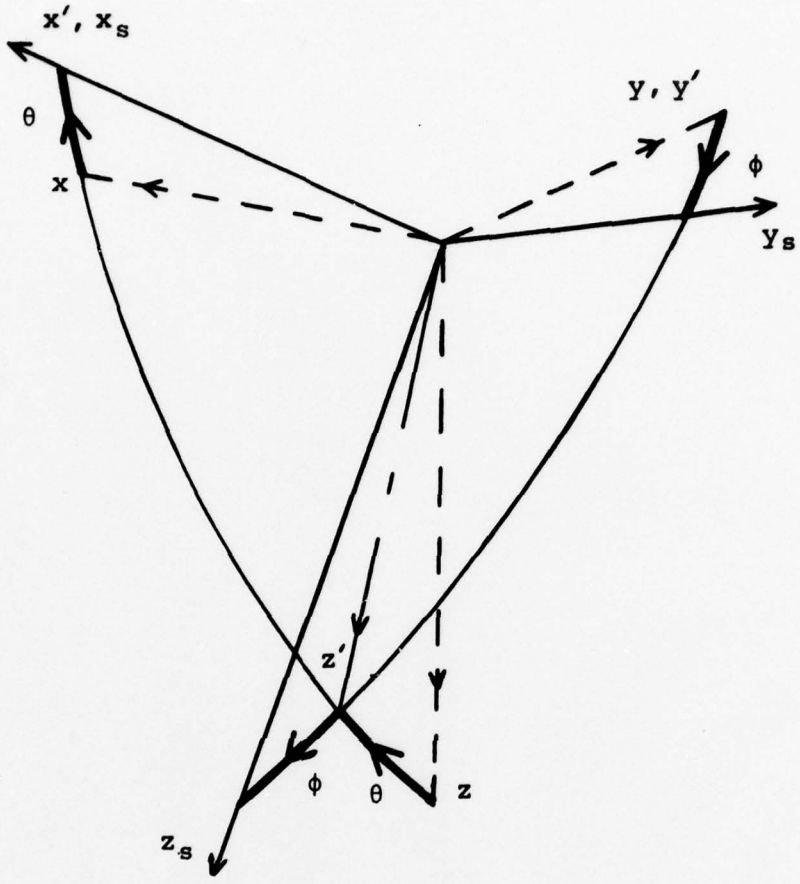

Fig.1 Angular orientation of cable element axes $x_s y_s z_s$ relative to cable axes xyz

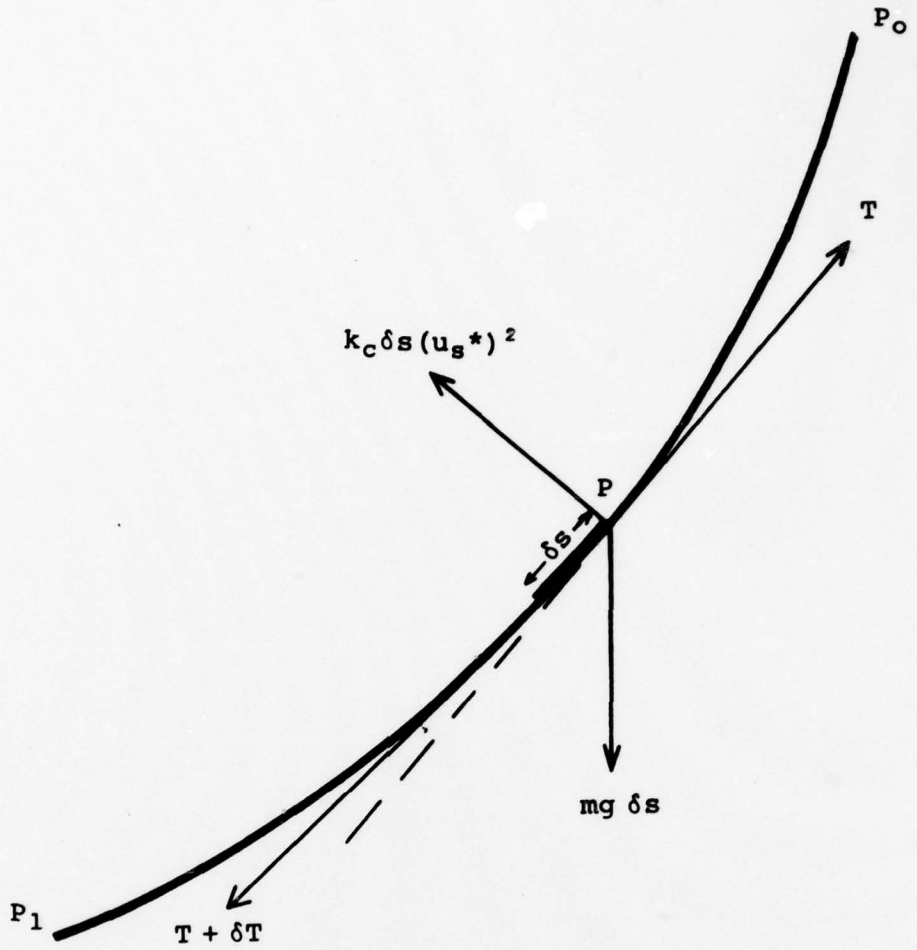

Fig.2 Forces acting on cable element (in vertical plane containing u_s^* at P)

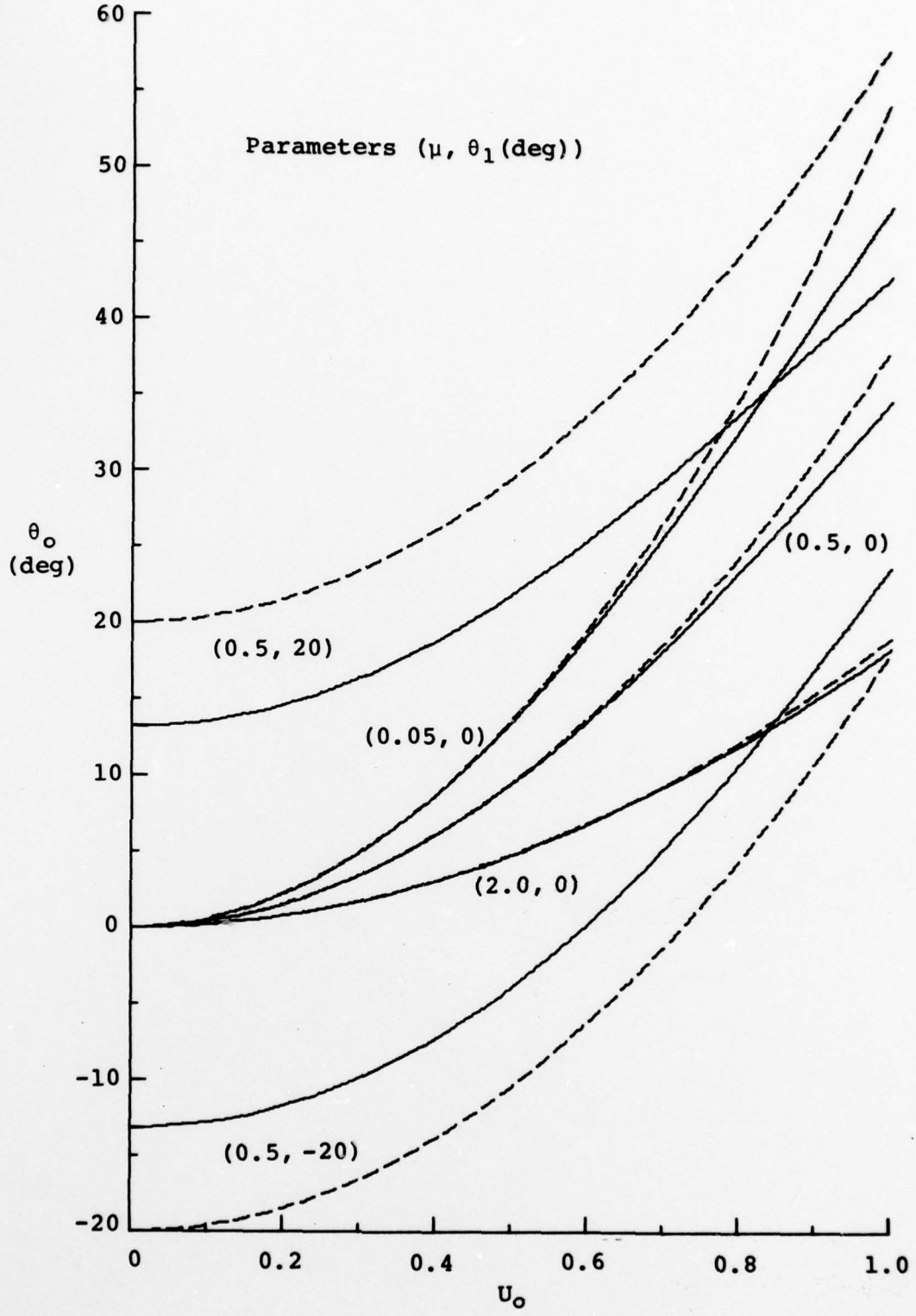

Fig.3 Comparison between two-dimensional 'general' (full line) and 'approximate' (broken line) solution of angular orientation for uniform fluid velocity; θ_o vs. U_o for parameters μ and θ_1

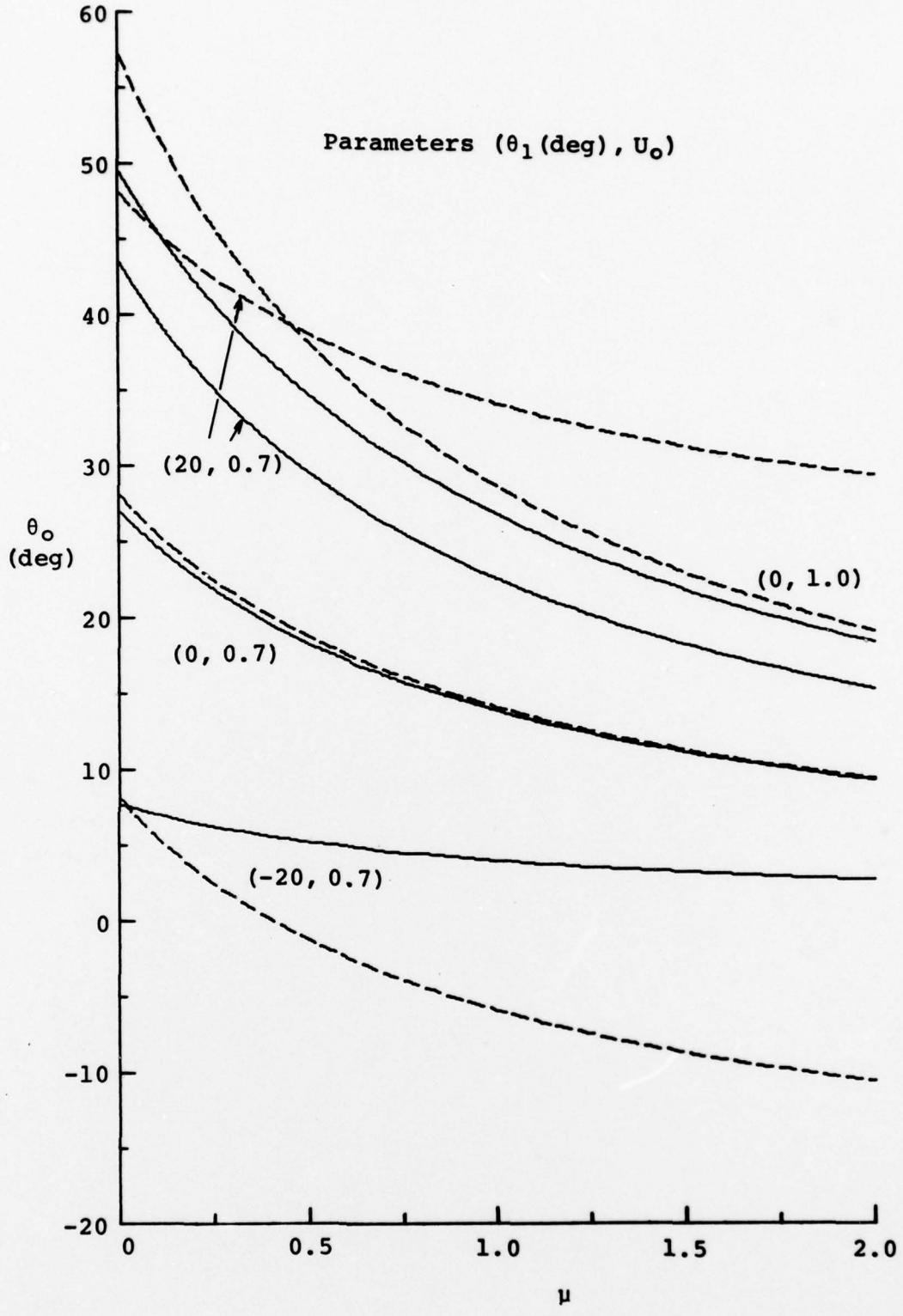

Fig.4 As Fig.3, but θ_o vs. μ for parameters θ_1 and U_o

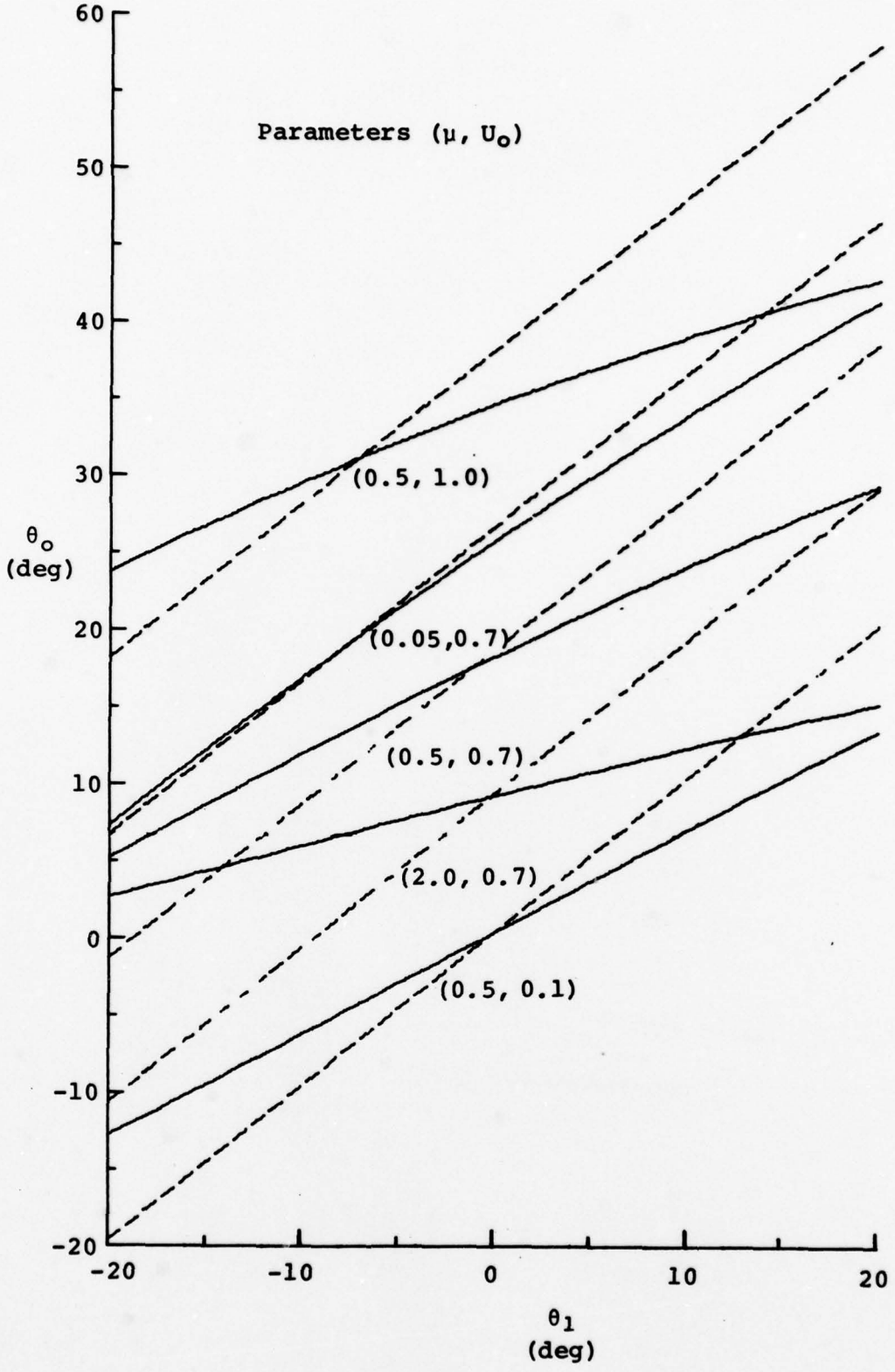

Fig.5 As Fig.3, but θ_o vs. θ_1 for parameters μ and U_o

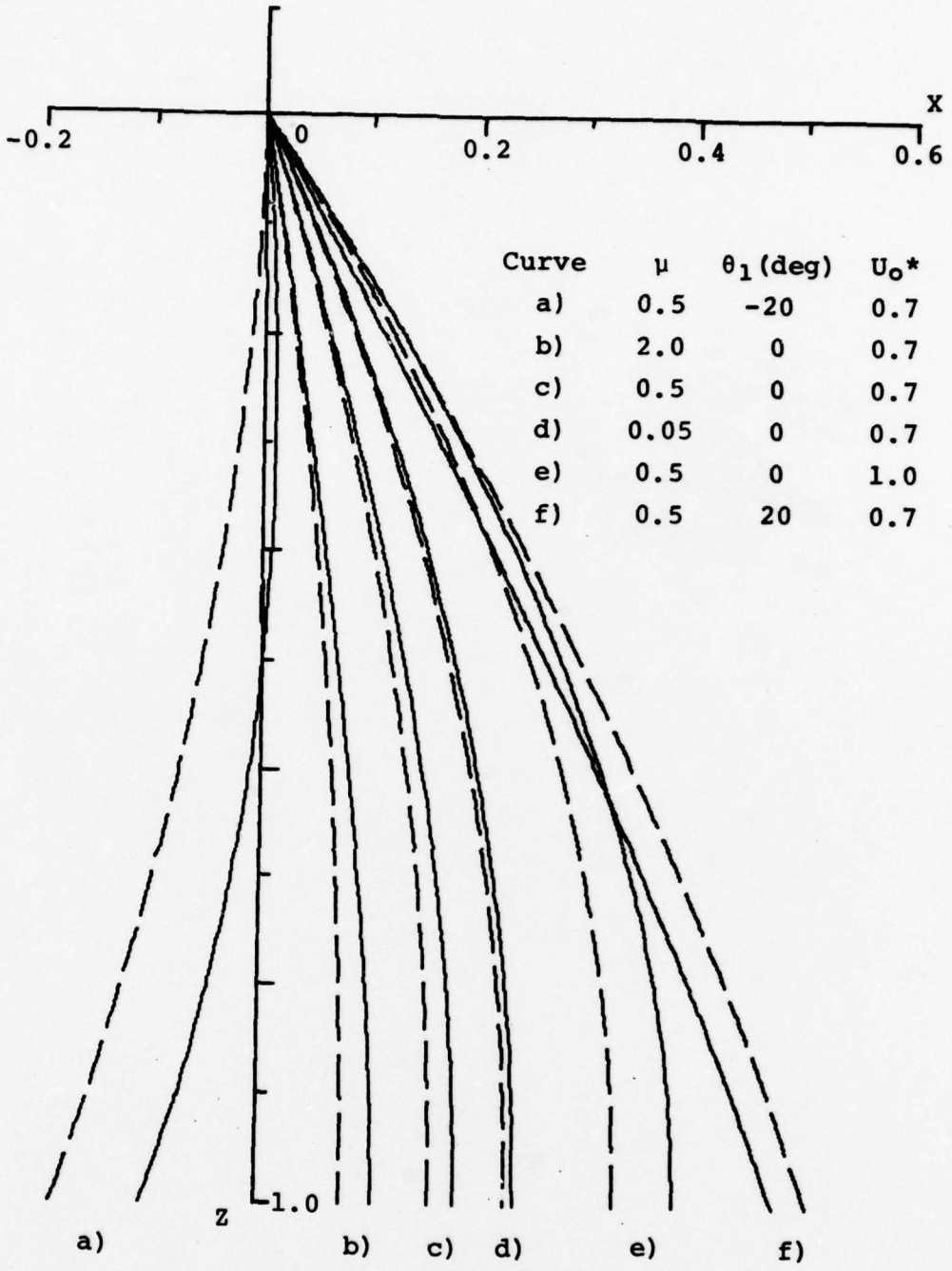

Fig.6 Comparison between cable shapes obtained using 'general' (full line) and 'approximate' (broken line) two-dimensional solution for uniform fluid velocity

a) independent variable ψ_o (deg)

$\chi_1 = \pm 180^o$

$\gamma_1 = 10^o$

$U_o^* = 0.7$

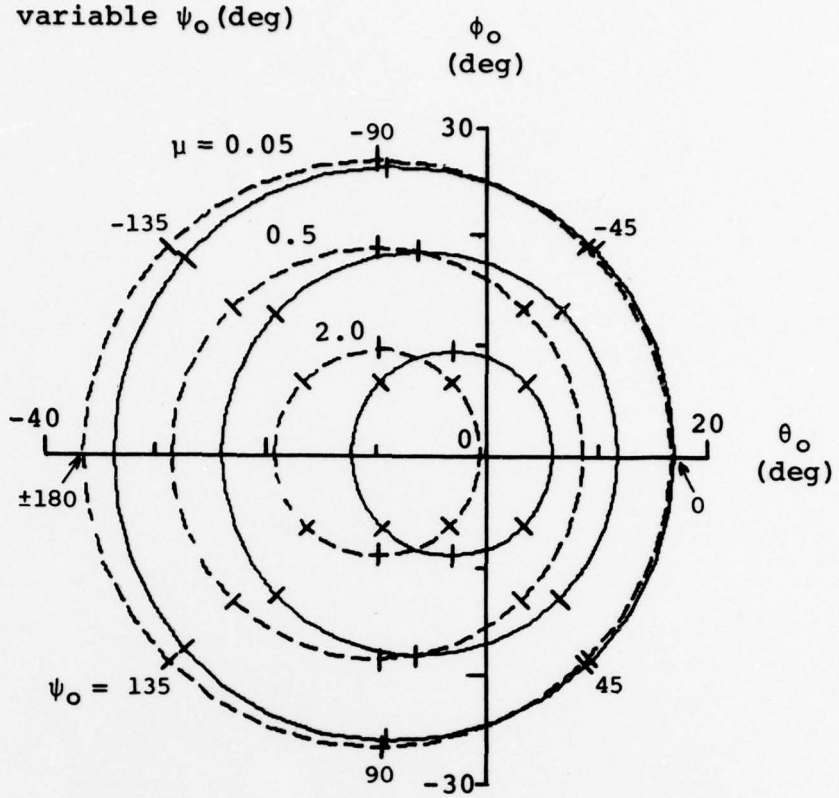

b) independent variable χ_1 (deg)

$\gamma_1 = 10^o$

$U_o^* = 0.7$

$\psi_o = 180^o$

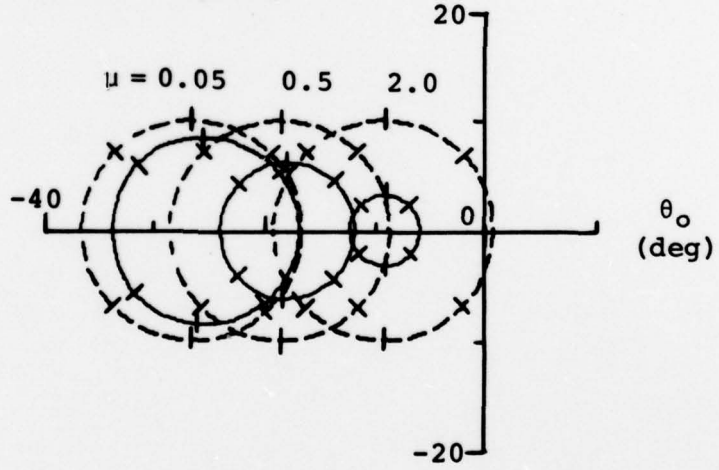

Fig.7 Comparison between three-dimensional 'general' (full line) and 'approximate' (broken line) solution of angular orientation in pitch and roll for uniform fluid velocity, parameter μ, and independent variable (a) ψ_o and (b) χ_1. In Figs.7 to 9, tick marks indicate equispaced values of the independent variable; values are shown only in Fig.7a, but are the same at corresponding circumference positions for each figure

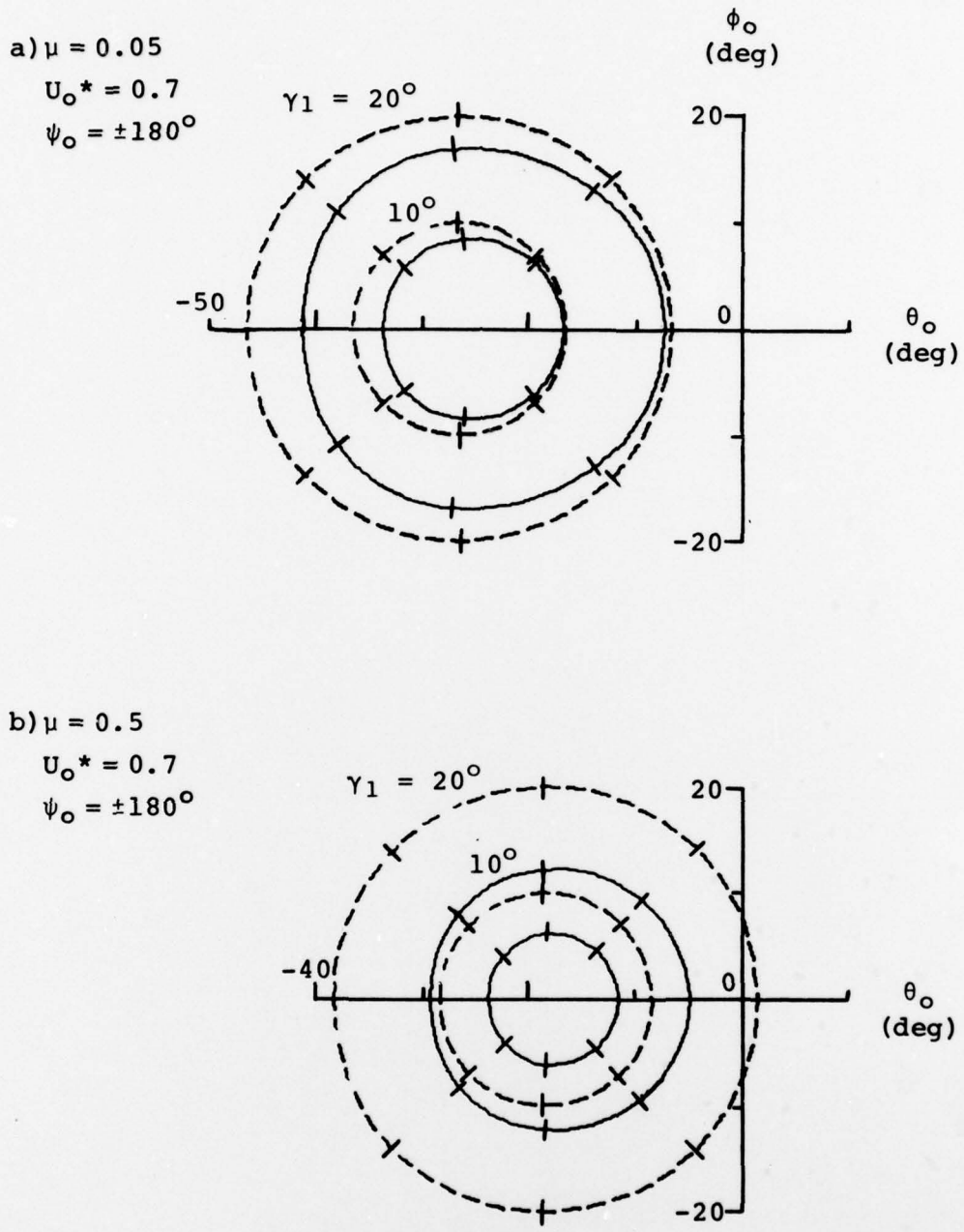

Fig.8 As Fig.7, but for parameter γ_1, independent variable χ_1, and (a) $\mu = 0.05$ and (b) $\mu = 0.5$

a) $\mu = 0.05$
$\gamma_1 = 10^\circ$
$\psi_o = \pm 180^\circ$

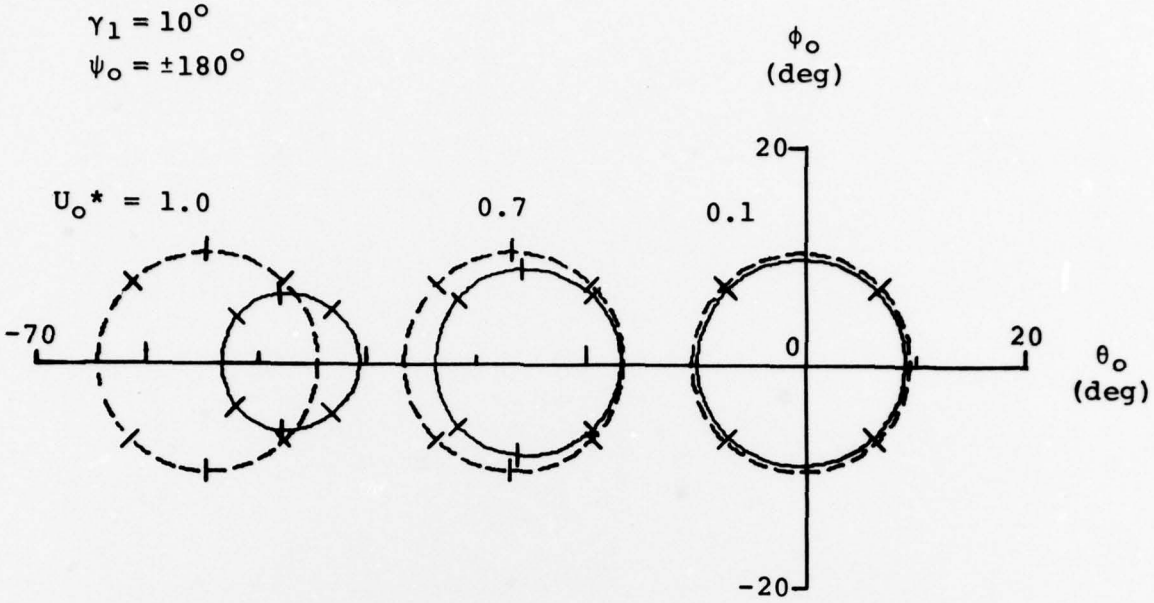

b) $\mu = 0.5$
$\gamma_1 = 10^\circ$
$\psi_o = \pm 180^\circ$

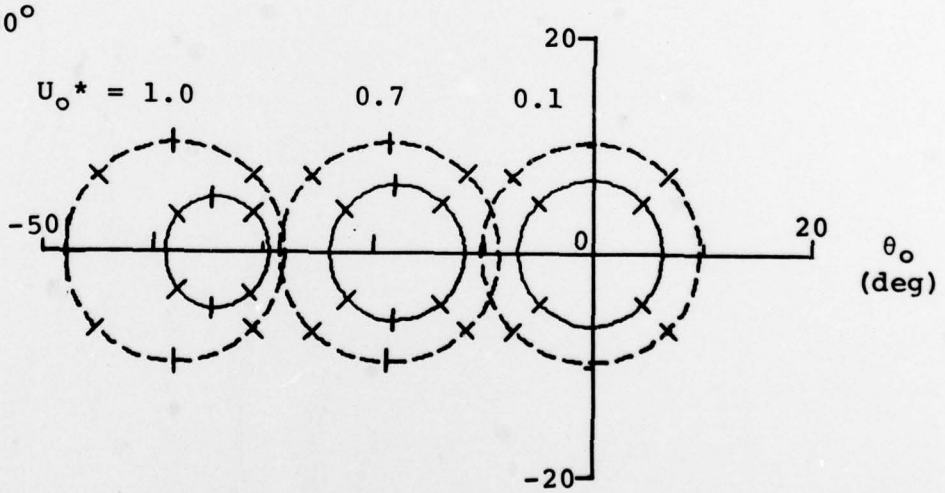

Fig.9 As Fig.8, but for parameter U_o^*

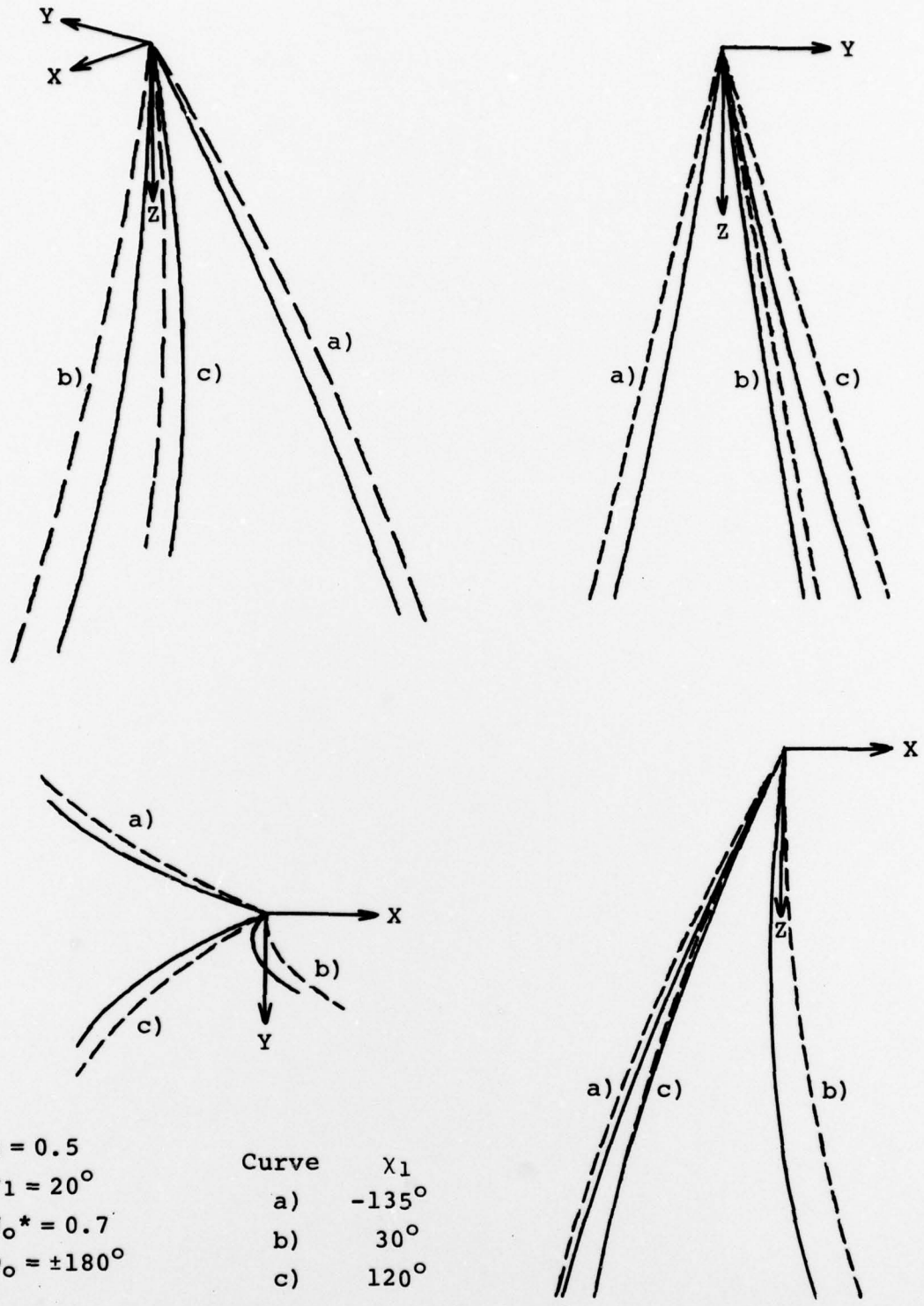

$\mu = 0.5$
$\gamma_1 = 20^\circ$
$U_o^* = 0.7$
$\psi_o = \pm 180^\circ$

Curve	χ_1
a)	-135°
b)	30°
c)	120°

Fig.10 Comparison between cable shapes obtained using 'general' (full line) and 'approximate' (broken line) three-dimensional solution for uniform fluid velocity. Four views of same shapes are shown

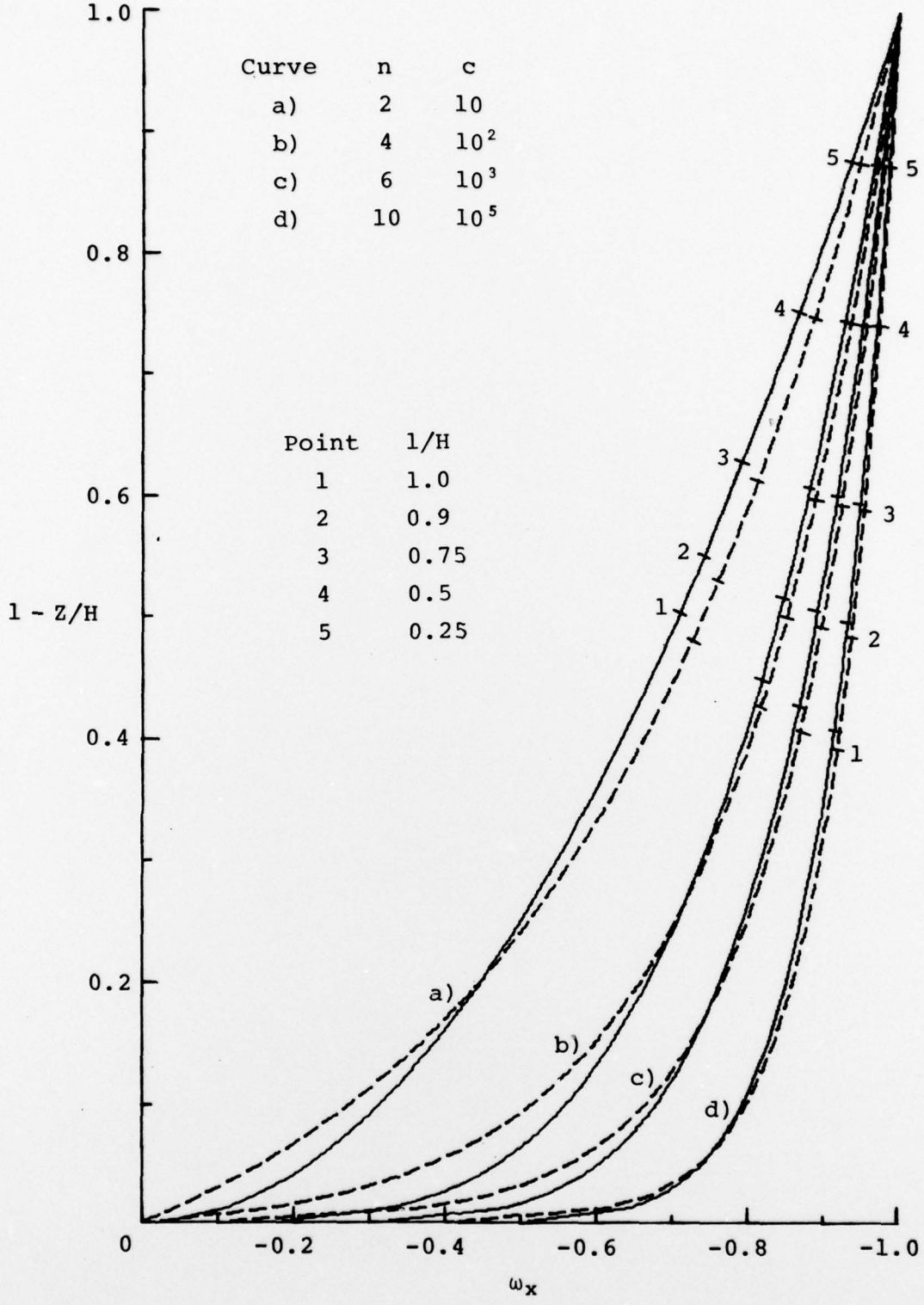

Fig.11 Velocity profiles for wind above the sea; power law (full line) for parameter n, and log law (broken line) for parameter c. Points at which $\langle\omega_x\rangle = \omega_x$ are shown for $\lambda_x = 0$ and parameter 1/H

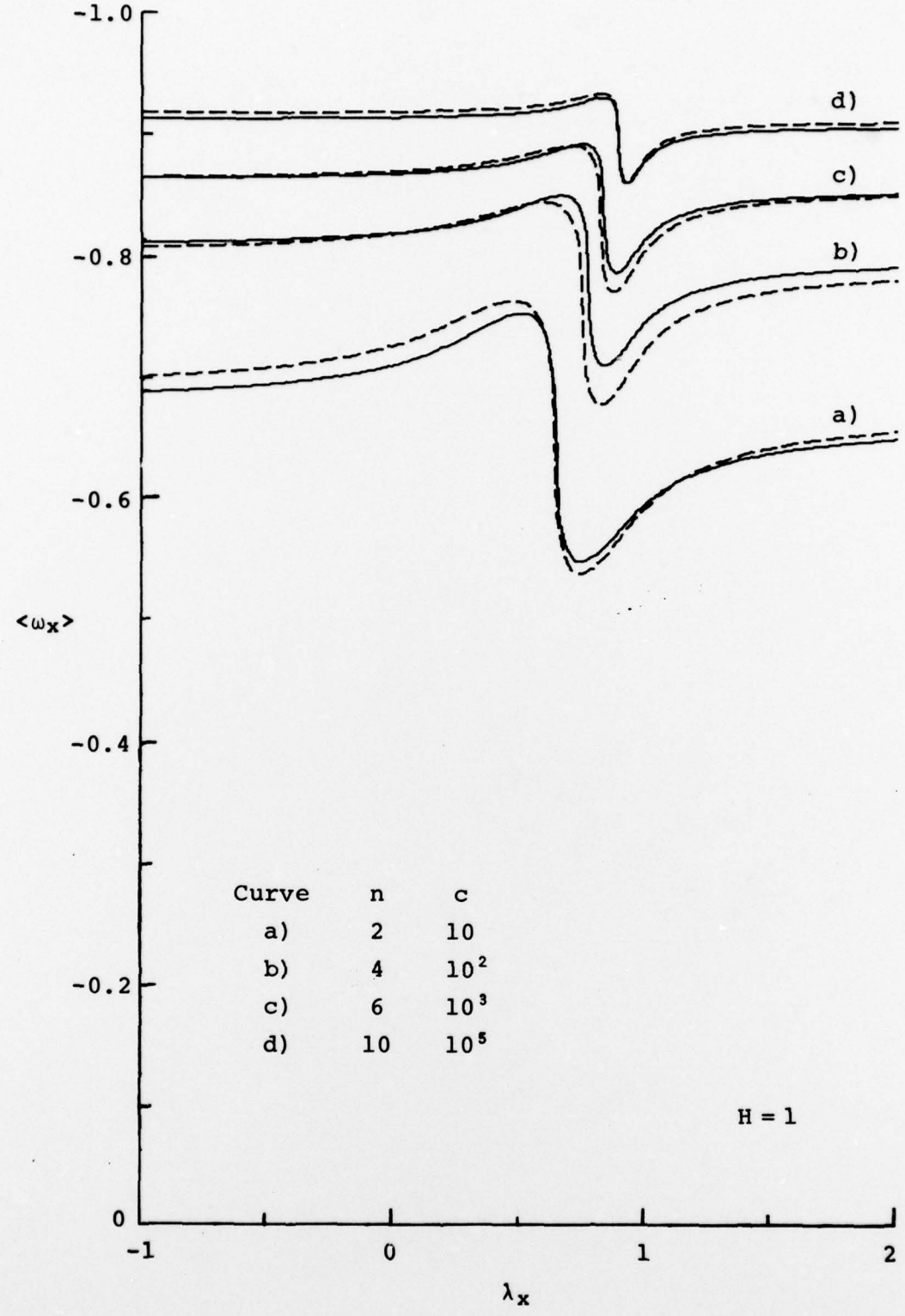

Fig.12 Equivalent mean fluid velocity for power (full line) and log (broken line) laws; $\langle\omega_x\rangle$ vs. λ_x for parameters n or c

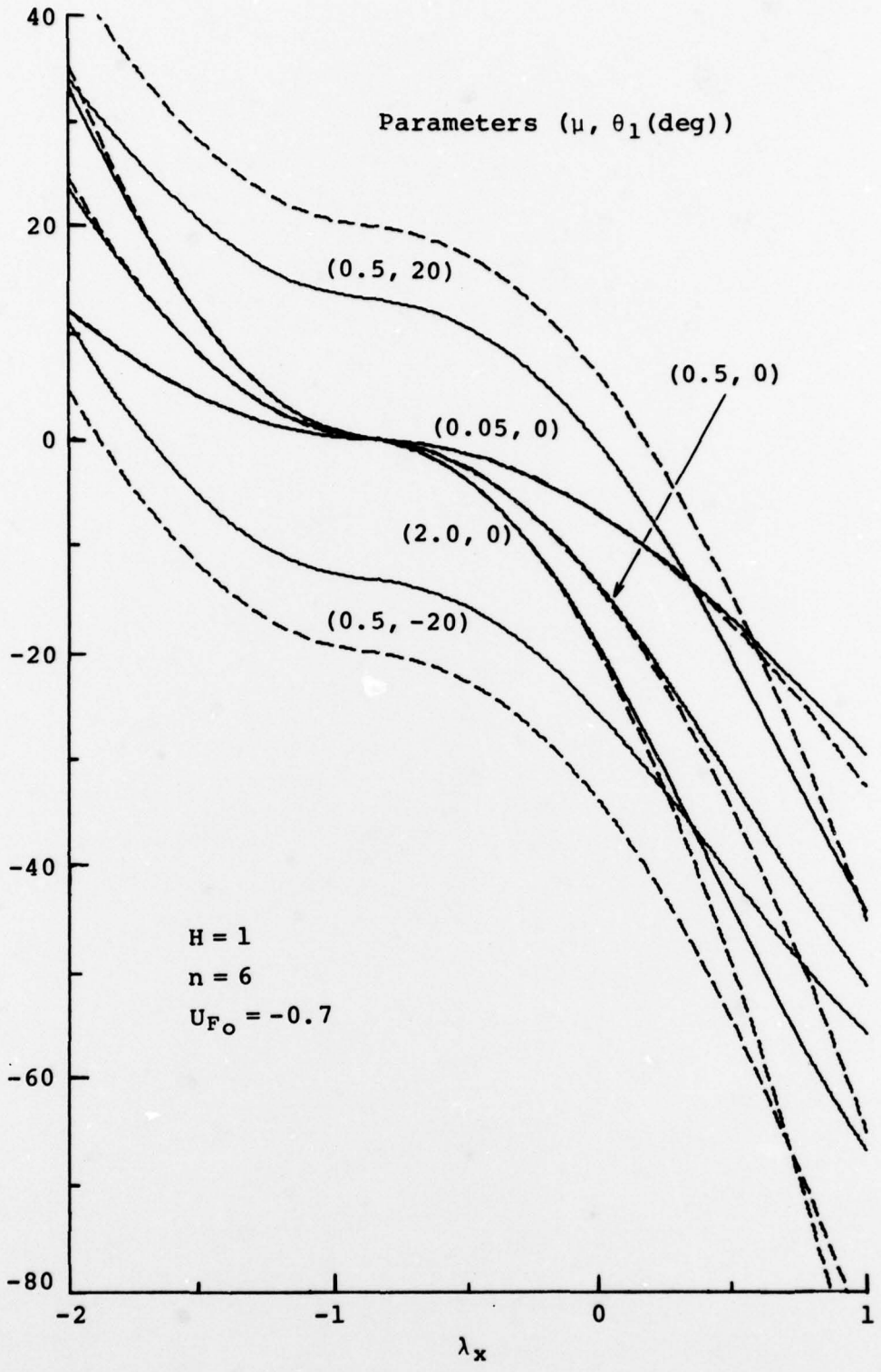

Fig.13 Comparison between two dimensional 'general' (full line) and 'approximate' (broken line) solution of angular orientation for power law with equivalent mean fluid velocity used in latter; θ_o vs. λ_x for parameters μ and θ_1

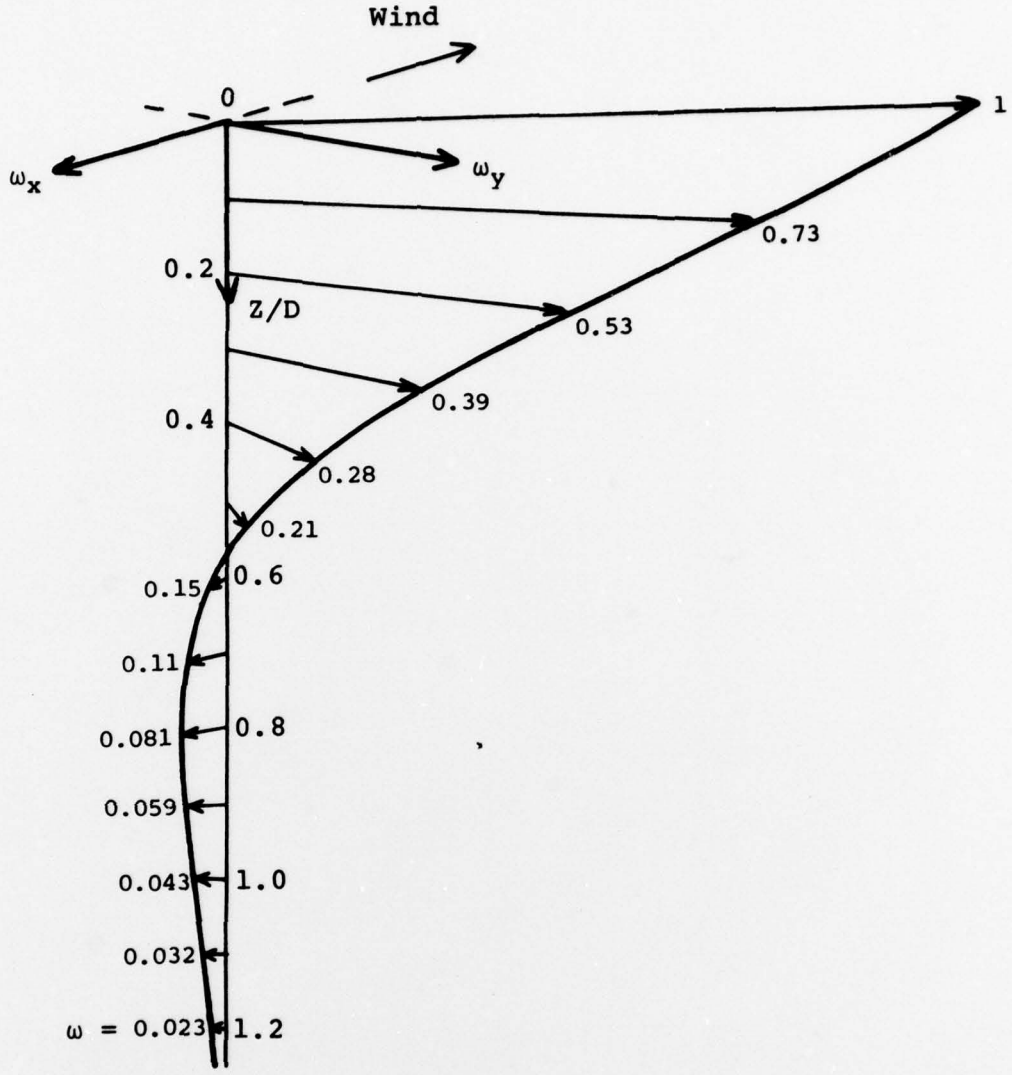

Fig.14 Ekman spiral velocity profile for sea current (viewed below sea level). Horizontal velocity vectors are shown at intervals in Z/D of 0.1

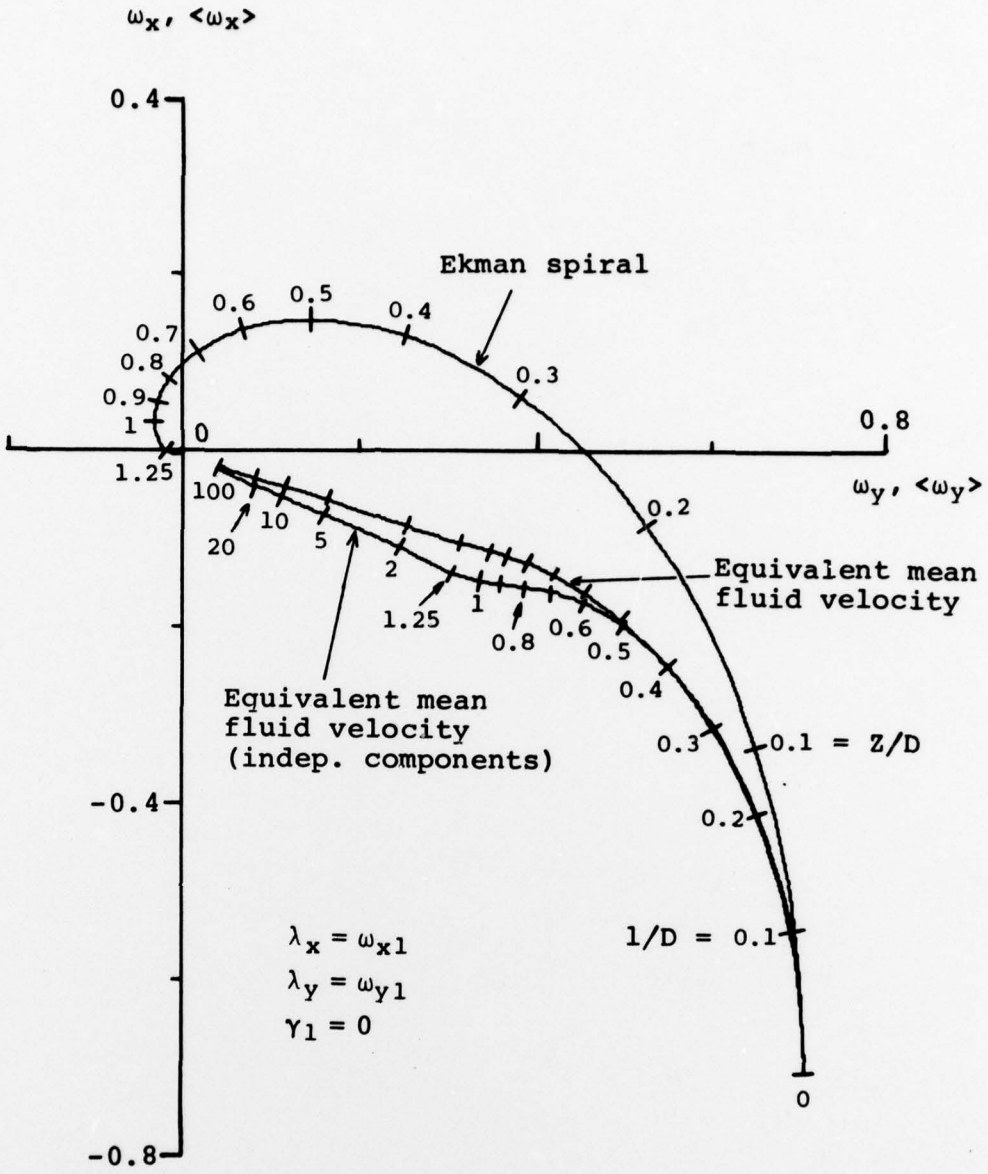

Fig.15 Ekman spiral (ω_x,ω_y) and equivalent mean fluid velocity ($\langle\omega_x\rangle$,$\langle\omega_y\rangle$) for independent variables Z/D and 1/D respectively (values shown beside tick marks). Equivalent mean fluid velocity calculated using 'independent velocity component assumption' is also shown

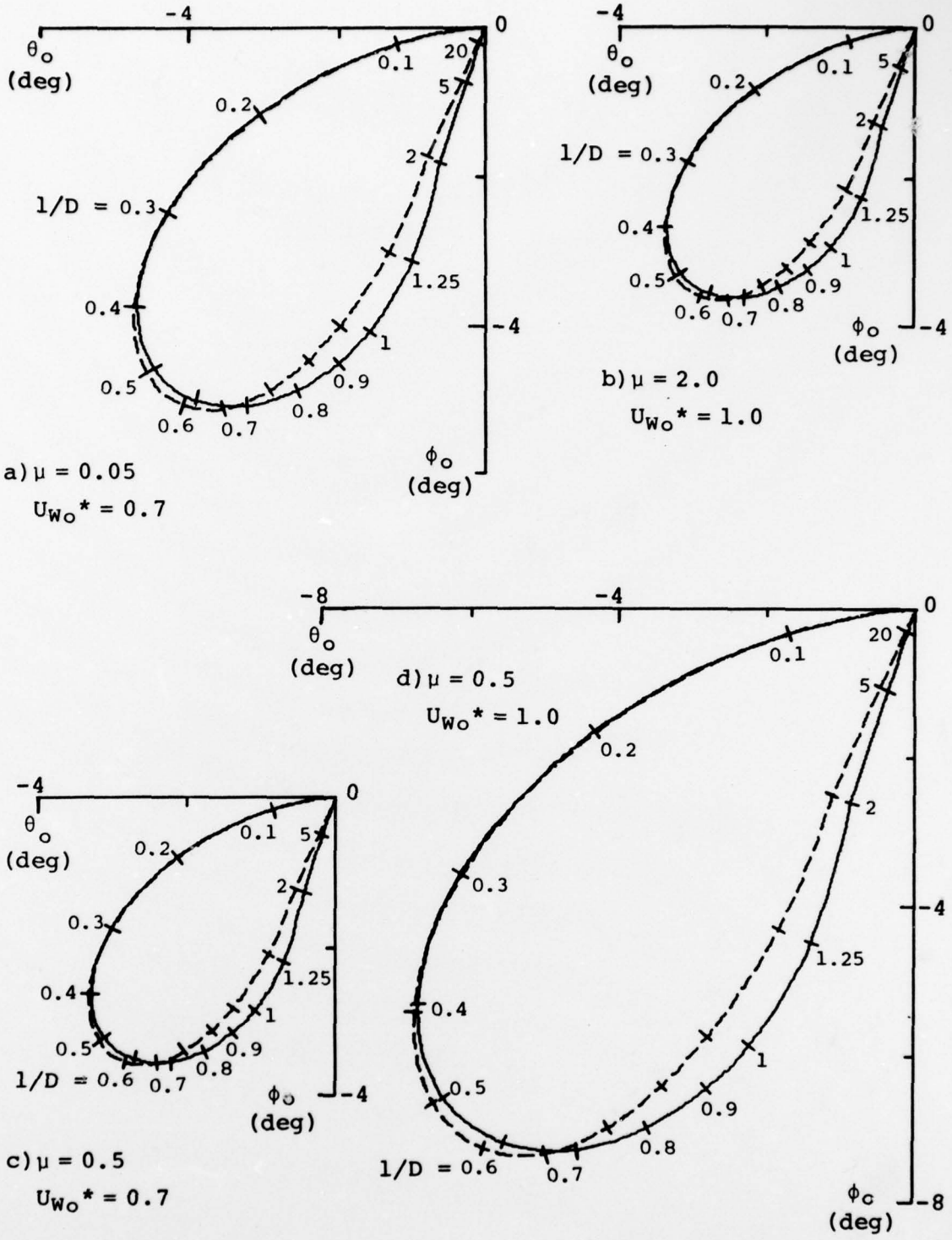

Fig.16 Three-dimensional 'approximate' solution (full line) of angular orientation in pitch and roll for Ekman spiral with parameter μ and U_{Wo}* and independent variable 1/D (values shown beside tick marks). Solution is also shown (broken line) using 'independent velocity component assumption'

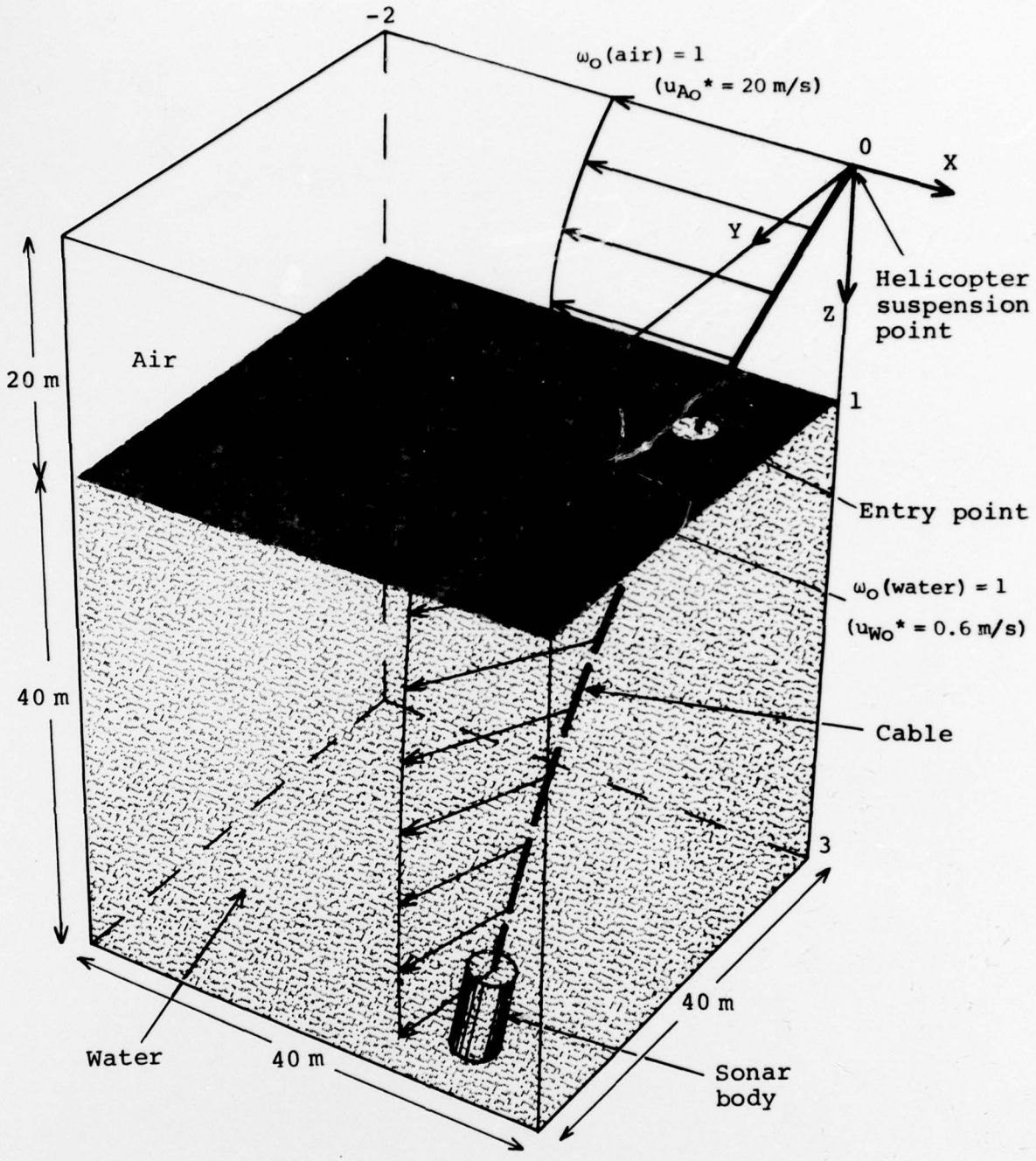

Fig.17 Example of sonar body suspended from a helicopter; note the difference in scales of the fluid velocity vectors for air and water

DOCUMENT CONTROL DATA SHEET

Security classification of this page: Unclassified

1. Document Numbers
   (a) AR Number: AR-001-269
   (b) Document Series and Number: Aerodynamics Report 149
   (c) Report Number: ARL-Aero-Report-149

2. Security Classification
   (a) Complete document: Unclassified
   (b) Title in isolation: Unclassified
   (c) Summary in isolation: Unclassified

3. Title: STEADY STATE BEHAVIOUR OF A CABLE USED FOR SUSPENDING A SONAR BODY FROM A HELICOPTER

4. Personal Author(s): N. E. Gilbert

5. Document Date: May 1978

6. Type of Report and Period Covered: Report

7. Corporate Author(s): Aeronautical Research Laboratories

8. Reference Numbers
   (a) Task: NAV 74/4
   (b) Sponsoring Agency: ARL File A2/19

9. Cost Code: 51 7740

10. Imprint: Aeronautical Research Laboratories, Melbourne

11. Computer Program(s) (Title(s) and language(s)):

12. Release Limitations (of the document): Approved for public release

12-0. Overseas:	No.		P.R.		A		B		C		D		E	

13. Announcement Limitations (of the information on this page): No limitation

14. Descriptors:

Cables (Ropes)	Helicopters	
Towing cables	Air towed sonar	
Mathematical models	Wind velocity	
	Ocean currents	

15. Cosati Codes: 1309, 1201, 2004

16.

ABSTRACT

A three-dimensional steady state mathematical model of a cable used to suspend a sonar body from a helicopter is derived. Results are presented in dimensionless form for a length of cable totally immersed in any Newtonian fluid, and may therefore be applied to a number of practical problems. Various approximations are made in order to obtain analytical solutions. The suitability of the approximations is investigated by comparing solutions of the general and approximate equations for a uniform fluid velocity. In general, where maximum angular deviations from the vertical are small, agreement is observed to be very good. Two-dimensional "power" and "log" laws are assumed for the wind above the sea, and a three-dimensional Ekman spiral is assumed for the sea current. For these non-uniform fluid velocities, the concept of an "equivalent mean fluid velocity" is used to simplify greatly the presentation of results.

DISTRIBUTION

	Copy No.
AUSTRALIA	
DEPARTMENT OF DEFENCE	
Central Office	
Chief Defence Scientist	1
Executive Controller, ADSS	2
Superintendent, Defence Science Administration	3
Australian Defence Scientific and Technical Representative (UK)	4
Counsellor, Defence Science (USA)	5
Defence Library	6
JIO	7
Assistant Secretary, DISB	8–23
Aeronautical Research Laboratories	
Chief Superintendent	24
Superintendent, Aerodynamics Division	25–26
Divisional File, Aerodynamics Division	27
Author—N. E. Gilbert	28–31
Library	32
D. C. Collis (for ABS–RW Group)	33
Materials Research Laboratories	
Librarian	34
Defence Research Centre	
Librarian	35
Chief Superintendent, Weapons Research Laboratory	36
Chief Superintendent, Advanced Engineering Laboratory	37
Central Studies Establishment Information Centre	
Librarian	38
Engineering Development Establishment	
Librarian	39
RAN Research Laboratory	
Librarian	40
Navy Office	
SO (Helicopter)	41
Naval Scientific Adviser	42
DNAE (Asst. Dir. Research)	43
O.I.C. AMAFTU (RANAS, Nowra)	44
O.I.C. Sea King Simulator (RANAS, Nowra)	45 & 143
Army Office	
Army Scientific Adviser	46
Royal Military College, Librarian	47
US Army Standardisation Group	48
Air Office	
Air Force Scientific Adviser	49
Aircraft Research and Development Unit	50
Engineering (CAFTS) Library	51
D. Air Eng.	52
H.Q. Support Command (SENGSO)	53

NETHERLANDS

National Aerospace Laboratory (NLR), Librarian		114

NEW ZEALAND

Air Department, RNZAF, Aero. Documents Section		115

Universities

Canterbury	Librarian	116

SWEDEN

Aeronautical Research Institute, Librarian		117

SWITZERLAND

Institute of Aerodynamics, E.T.H.		118

UNITED KINGDOM

Aeronautical Research Council, N.P.L. (Secretary)		119
CAARC, N.P.L. (Secretary)		120
Royal Aircraft Establishment, Librarian, Farnborough		121
Royal Aircraft Establishment, Librarian, Bedford		122
British Library, Science Reference Library		123

Aircraft Companies

Westland Helicopters Ltd:	Chief Defence Scientist	124
	Mr B. Pitkin, Chief Flight Mech. Engr	125

Universities and Colleges

Bristol	Librarian, Engineering Department	126
Cambridge	Librarian, Engineering Department	127
Liverpool	Professor J. H. Preston, Fluid Mech. Dept.	128
London	Professor A. D. Young, Queens College	129
Manchester	Professor, Applied Mathematics	130
	Professor N. Johannessen	131
Nottingham	Librarian	132
Southampton	Librarian	133
Cranfield Institute of Technology	Professor of Aeronautical Engineering	134

UNITED STATES OF AMERICA

NASA Scientific and Technical Information Facility		135
American Institute of Aeronautics and Astronautics		136
Applied Mechanics Reviews		137
United Technologies Corporation, Fluid Dynamics Labs		138

Universities and Colleges

Cornell (New York)	Librarian, Aeronautical Laboratories	139
Johns Hopkins	Professor S. Corrsin, Dept. of Mech. Eng.	140
Stanford	Librarian, Department of Aeronautics	141
California Institute of Technology	Librarian, Guggenheim Aero. Labs	142

Spares 144–153